Published for SISSA by Springer

Received: *January 20, 2026*
Accepted: *June 19, 2026*
Published: *August 6, 2026*

Measurement of the Zγ production cross section and search for anomalous neutral triple gauge couplings in pp collisions at $\sqrt{s} = 13$ TeV

The CMS collaboration

Full author list at the end of the paper

E-mail: cms-publication-committee-chair@cern.ch

Abstract: A measurement of the fiducial cross section of the associated production of a Z boson and a high-p_{T} photon, where the Z decays to two neutrinos, and a search for anomalous triple gauge couplings are reported. The results are based on data collected by the CMS experiment at the LHC in proton-proton collisions at $\sqrt{s} = 13$ TeV during 2016–2018, corresponding to an integrated luminosity of 138 fb^{-1}. The fiducial Zγ cross section, where a photon with a p_{T} greater than 225 GeV is produced in association with a Z, and the Z decays to a $\nu\bar{\nu}$ pair ($\mathrm{Z}(\nu\bar{\nu})\gamma$), is measured to be $23.3^{+1.4}_{-1.3}$ fb, in agreement, within uncertainties, with the standard model prediction. The differential cross section as a function of the photon p_{T} has been measured and compared with standard model predictions computed at next-to-leading and at next-to-next-to-leading order in perturbative quantum chromodynamics. Constraints have been placed on the presence of anomalous couplings that affect the ZZγ and Zγγ vertex using the p_{T} spectrum of the photons. The observed 95% confidence level intervals for CP-conserving h_3^{γ} and h_4^{γ} are determined to be $(-3.4, 3.5)\times10^{-4}$ and $(-6.8, 6.8)\times10^{-7}$, and for h_3^{Z} and h_4^{Z} they are $(-2.2, 2.2)\times10^{-4}$ and $(-4.1, 4.2)\times10^{-7}$, respectively. These are the strictest limits to date on h_3^{γ}, h_3^{Z} and h_4^{Z}.

Keywords: Beyond Standard Model, Hadron-Hadron Scattering, Particle and Resonance Production, Photon Production

ArXiv ePrint: 2601.14102

https://doi.org/10.1007/JHEP08(2026)049

JHEP08(2026)049

Contents

1 Introduction

Measurements of the production cross sections of electroweak (EW) dibosons at collider experiments provide important tests of the electroweak sector of the standard model (SM). In the SM, vertices with three neutral electroweak bosons (ZZZ, Zγγ, and ZZγ) are not allowed at the tree level, as they violate the $SU(2)_L \times U(1)_Y$ symmetry. However, in the presence of new physics, anomalous neutral triple gauge couplings (aNTGCs) could arise that can be introduced as extension to the SM using the Lagrangian terms of all possible Lorentz structures, or in an effective field theory, where the operators have dimensions higher than those of the SM electroweak Lagrangian [1].

To estimate these effects, vertex functions have been calculated in refs. [1–3] to describe the most general Lorentz- and $U_Y(1)$-invariant interactions of an incoming off-shell Z boson or photon, and an outgoing on-shell Z with a photon (figure 1). The strength of this interaction is determined by four parameters: h_1^V and h_2^V, which are CP violating, and h_3^V and h_4^V, which are CP conserving. As an example, the ZZγ vertex function (in the case of outgoing

JHEP08(2026)049

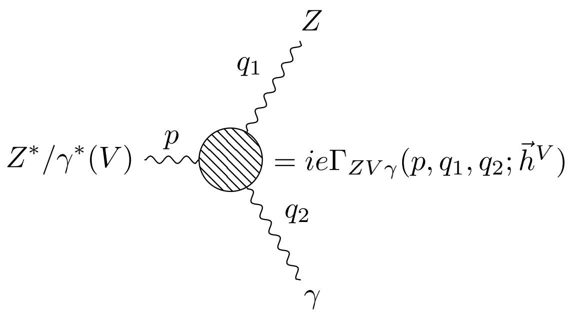

Figure 1. The Feynman diagram for the ZVγ vertex, where V $= \gamma^*/\mathrm{Z}^*$, in the presence of an aNTGC.

on-shell Z/γ) is defined as:

$$\Gamma^{\alpha\beta\mu}_{\mathrm{ZZ}\gamma} = \frac{p^2 - q_1^2}{m_\mathrm{Z}^2}\left[h_1^\mathrm{Z}(q_2^\mu g^{\alpha\beta} - q_2^\alpha g^{\mu\beta}) + \frac{h_2^\mathrm{Z}}{m_\mathrm{Z}^2} p^\alpha \left[(p \cdot q_2) g^{\mu\beta} - q_2^\mu p^\beta\right]\right.$$
$$\left. + h_3^\mathrm{Z} \epsilon^{\mu\alpha\beta\rho} q_{2\rho} + \frac{h_4^\mathrm{Z}}{m_\mathrm{Z}^2} p^\alpha \epsilon^{\mu\beta\rho\sigma} p_\rho q_{2\sigma}\right], \tag{1.1}$$

where $\Gamma^{\alpha\beta\mu}_{Z\gamma\gamma}$ can be obtained with the replacements:

$$\frac{p^2 - q_1^2}{m_\mathrm{Z}^2} \to \frac{p^2}{m_\mathrm{Z}^2} \text{ and } h_i^\mathrm{Z} \to h_i^\gamma.$$

Here, $g^{\alpha\beta}$ denotes the Minkowski metric tensor with signature $(+, -, -, -)$, and $\epsilon^{\mu\alpha\beta\rho}$ is the totally antisymmetric Levi-Civita tensor, defined such that $\epsilon_{0123} = +1$, and repeated indices are summed over the four space-time coordinates $(0, 1, 2, 3)$.

The existence of such an effective vertex can be detected as either an excess, or as a deficit relative to the SM prediction in the kinematic distributions of the Zγ production, since the aNTGC introduces an additional channel for this process (figure 2), changing the cross section to $\sigma_\text{total} = \sigma_\text{SM} + \sigma_\text{interference} + \sigma_\text{aNTGC}$ [3]. In the presence of aNTGCs, the total production cross section of the Zγ process depends on the strength of the couplings. The leading-order corrections to the SM cross-section scale linearly with the CP-conserving couplings due to the interference between the SM and aNTGC amplitudes, while second-order corrections arise from terms quadratic in these strengths. In contrast, the CP-violating couplings do not interfere with either the SM amplitude or an anomalous CP-conserving amplitude, and their impact on the Lagrangian is manifested only at the quadratic level [4]. However, when the outgoing photon has a high transverse momentum, the interference term becomes negligible and the Lagrangian associated with the CP-conserving couplings becomes, as it is for the CP-violating couplings, quadratically sensitive [5]. At energies exceeding a few hundred GeV, the limits on h_1^V and h_2^V become comparable to those on h_3^V and h_4^V, respectively, and consequently in this paper only a search of the CP-conserving couplings h_3^V and h_4^V is reported.

In the analysis presented here, we have used the vertex function approach, to enable comparison with previous results. While not considered in this paper, a new formalism that

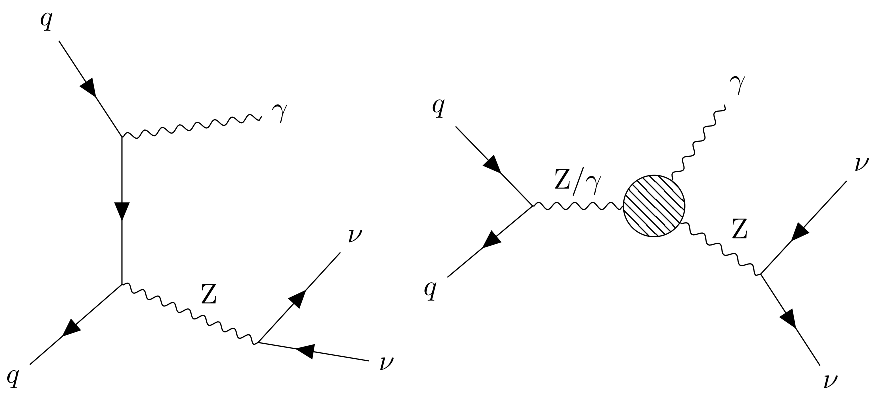

Figure 2. The leading-order Feynman diagram for SM Zγ production in the t-channel (left), and (right) the additional diagram for the beyond SM s-channel Zγ production due to the presence of aNTGCs.

includes contributions from off-shell decays $Z^* \to \nu\bar{\nu}$ has been presented in [6], and a method to compare the two frameworks can be found in [7].

The neutral decay of the Z boson ($Z \to \nu\bar{\nu}$) is the most suitable channel to detect aNTGCs, as it provides a clean final state signature with a 20% branching fraction, compared to the charged lepton decay channel where it is 10%. The hadronic decay channel of the Z boson has the highest branching fraction of 70%, but also has a much larger background from γ+jets events.

Measurements of the production cross section of $Z(\nu\bar{\nu})\gamma$ in hadron collisions and studies of the triple ZZγ and Zγγ vertices were first performed by the D0 Collaboration [8], and subsequently by the CDF [9, 10], CMS [11, 12], and ATLAS [13, 14] Collaborations. In addition, limits on the anomalous couplings have been set in the charged-lepton final state $Z(\ell^+\ell^-)\gamma$, where ℓ = e, μ, by the D0, CDF, ATLAS, and CMS Collaborations [8–10, 12, 15, 16].

We report here a search for aNTGCs (ZZγ and Zγγ) with a high-p_T photon and a large missing momentum. and a measurement of the production cross section of the Zγ process in data collected by the CMS experiment in proton-proton (pp) collisions at $\sqrt{s} = 13\,\text{TeV}$ during 2016–2018, corresponding to an integrated luminosity of $138\,\text{fb}^{-1}$.

In this paper the CMS detector is described in section 2 and the analysis strategy in section 3. The data sets and the simulated samples used to model the signal and the backgrounds are described in section 4. The criteria used to select physics objects and to define the signal and control regions are described in sections 5 and 6, and in section 7 the methods used to estimate the backgrounds are discussed. The procedures used to estimate the systematic uncertainties that affect the modeling are described in section 8. The methods used to estimate the overall uncertainty of the obtained results are described in sections 9 and 10. Tabulated results are provided in the HEPData record for this analysis [17].

2 The CMS detector and object reconstruction

The CMS apparatus [18, 19] is a multipurpose, nearly hermetic detector, designed to trigger on [20–22] and identify electrons, muons, photons, and (charged and neutral) hadrons [23–25]. The central feature of the CMS apparatus is a superconducting solenoid of 6 m internal diameter, providing a magnetic field of 3.8 T. A silicon pixel and strip tracker, a lead tungstate crystal electromagnetic calorimeter (ECAL) with a silicon strip preshower detector (ES) placed at the front faces of the two endcap calorimeters, and a brass and scintillator hadron calorimeter (HCAL), each composed of a barrel and two endcap sections, are installed inside the solenoid. Avalanche photodiodes (APDs) are used to readout the barrel section of the ECAL (EB), while vacuum photo-triodes are used to readout the ECAL endcaps (EE). Forward calorimeters extend the η coverage provided by the barrel and endcap detectors, where η is the pseudorapidity and is defined using the polar angle θ as $\eta = -\ln[\tan(\theta/2)]$. Muons are detected in gas-ionization chambers embedded in the steel flux-return yoke outside the solenoid. A more detailed description of the CMS detector, together with a definition of the coordinate system and the relevant kinematic variables, can be found in ref. [18].

Events of interest are selected using a two-tier trigger system. The first level, composed of custom hardware processors, uses information from the calorimeters and muon detectors to select events at a rate of around 100 kHz within a fixed latency of about 4 μs [20]. The second level, known as the high-level trigger, consists of a farm of processors running a version of the full event reconstruction software optimized for fast processing and reduces the event rate to around 1 kHz before data storage [21, 22].

The global event reconstruction (also called particle-flow event reconstruction [26]) aims to reconstruct and identify each individual particle in an event, with an optimized combination of all subdetector information. In this process, the identification of the particle type (photon, electron, muon, charged hadron, neutral hadron) plays an important role in the determination of the particle direction and energy. Photons (e.g. coming from π^0 decays or from electron bremsstrahlung) are identified as ECAL energy clusters not linked to the extrapolation of any charged particle trajectory to the ECAL. Electrons (e.g. coming from photon conversions in the tracker material or from B hadron semileptonic decays) are identified as a primary charged particle track and potentially many ECAL energy clusters corresponding to this track extrapolation to the ECAL and to possible bremsstrahlung photons emitted along the way through the tracker material. Muons (e.g. from B hadron semileptonic decays) are identified as tracks in the central tracker consistent with either a track or several hits in the muon system, and associated with calorimeter deposits compatible with the muon hypothesis. Charged hadrons are identified as charged particle tracks neither identified as electrons, nor as muons. Finally, neutral hadrons are identified as HCAL energy clusters not linked to any charged hadron trajectory, or as a combined ECAL and HCAL energy excess with respect to the expected charged hadron energy deposit. The primary vertex (PV) is taken to be the vertex corresponding to the hardest scattering in the event, evaluated using tracking information alone, as described in section 9.4.1 of ref. [27].

Hadronic jets are clustered from all the PF candidates in an event using the infrared and collinear-safe anti-k_T algorithms [28, 29] with a distance parameter of 0.4. Jet momentum is determined as the vector sum of all particle momenta in the jet. From simulation, this is

JHEP08(2026)049

found to be on average within 5 to 10% of the true momentum over the whole p_T spectrum and detector acceptance. Additional pp interactions within the same, or nearby bunch crossings (pileup) can contribute energy depositions in the calorimeter and additional tracks, increasing the apparent jet momentum. To mitigate this effect, tracks identified as originating from pileup vertices are discarded and a correction is applied to account for any residual contributions [30].

Corrections to the jet energy are derived from simulation studies and applied so that the average measured jet energy is identical to particle level jets. *In situ* measurements of the momentum balance in dijet, γ+jet, Z+jet, and multijet events are used to determine any residual differences between the jet energy scale in the observed events and in simulation, and corrections factors are applied [31].

The missing transverse momentum vector $\vec{p}_T^{\text{miss}}$ is defined as the projection onto the plane perpendicular to the beam axis of the negative vector sum of the momenta of all reconstructed particle-flow objects in an event. Its magnitude is referred to as p_T^{miss} [32]. The $\vec{p}_T^{\text{miss}}$ vector is modified to account for corrections to the energy scale of the reconstructed jets.

For leptons, corrections are applied as weights to the simulated events to account for differences between data and simulation in the muon and electron reconstruction efficiencies. These corrections are determined using the "tag-and-probe" technique [33] with $Z \to e^+e^-$ events. Differences between the muon momentum scale in data and simulation are corrected for using a calibration derived in $Z \to \mu^+\mu^-$ events [24, 34]. An additional resolution smearing is included in the simulation to match the resolution in data. Similarly, scale and resolution corrections are applied to simulated electrons and photons to better match the energy scale and resolution measured in the data.

Spurious high-p_T^{miss} events can be due to a variety of reconstruction failures, detector malfunctions, or non-collision backgrounds. Such events are rejected by event filters designed to identify more than 85% of the spurious high-p_T^{miss} events, with a mistagging rate of less than 0.1% [32].

3 Analysis strategy

The signature of $Z(\nu\bar{\nu})\gamma$ events is a high-p_T photon associated with large p_T^{miss}. Figure 3 shows the generator-level photon p_T spectrum for different values of the anomalous coupling parameters. The sensitivity to aNTGCs increases with the photon p_T, with the greatest sensitivity above $p_T \approx 500\,\text{GeV}$. To better constrain all the SM background contributions to this process, we require events to have a photon with a p_T greater than 200 GeV. To select these high-p_T photons and to distinguish them from jets a dedicated identification algorithm, described in section 5, has been specifically developed for this analysis.

Backgrounds to the $Z(\nu\bar{\nu})\gamma$ process come from two main sources: one is the process $W \to e\bar{\nu}_e$, where the electron is reconstructed as a photon due to an inefficiency of the pixel tracker that contributes approximately 43% to the total background, and the $W(\ell\bar{\nu}_\ell)\gamma$ process, where the lepton is not identified, contributes around 33% of the total background. Both these background sources are estimated from data using control samples. Other smaller backgrounds are events with a photon coming from the processes $Z/\gamma^*(\ell^+\ell^-)\gamma$, $t\bar{t}\gamma$, $WV\gamma$, and $t+\gamma$, or with a final-state radiation photon in diboson or W production. The contributions

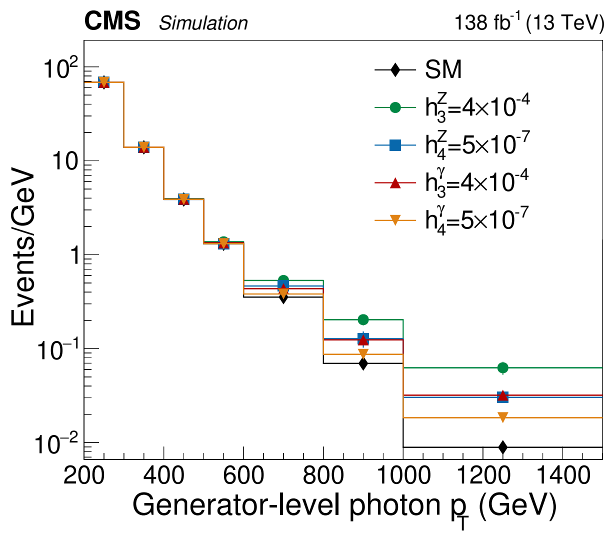

Figure 3. The generator-level photon p_{T} spectrum for various values of aNTGC couplings and the SM predictions.

from these processes are estimated using simulation to be 16% to the total background. An additional background contribution, where a jet is misidentified as a photon in association with large $p_{\mathrm{T}}^{\mathrm{miss}}$, is estimated from data to be 4% of the total background.

Direct ionization of the APDs [35] in EB, spikes, and bremsstrahlung radiation from beam-halo muons [36] in both EB and EE can mimic high-p_{T} photons and contribute approximately 4% to the total background.

4 Dataset and simulation

Samples of simulated data are used to model the background processes and to estimate the SM and aNTGC signals. These samples are produced using MadGraph5_aMC@NLO [37] v2.6.5 at QCD and EW leading order (LO), with up to 2 additional jets using the CP5 [38] underlying event PYTHIA v8.240 [39] tune. PYTHIA is used for fragmentation and hadronization and the detector response is simulated with the Geant4 package [40].

Correction factors (K-factors) that depend on the p_{T} of the photon are applied to account for next-to-next-to-leading order (NNLO) in QCD [41] and at next-to-leading order (NLO) in EW theory [42, 43]. In these references, the NLO EW K-factors for $\mathrm{Z}(\nu\bar{\nu})\gamma$ and $\mathrm{W}(\ell\bar{\nu}_\ell)\gamma$ were calculated for $\sqrt{s} = 14\,\mathrm{TeV}$, and have been recalculated for $\sqrt{s} = 13\,\mathrm{TeV}$ using the NNPDF31luxQED [44] PDF set. For the SM $\mathrm{Z}(\nu\bar{\nu})\gamma$ sample events where the photon p_{T} exceeds 200 GeV, at $\sqrt{s} = 13\,\mathrm{TeV}$, the QCD K-factors decrease from 1.55 to 1.2, while the EW K-factors decrease from 0.95 to 0.3 for the p_{T} range of 200–2000 GeV. For the $\mathrm{W}(\ell\nu_\ell)\gamma$ samples the QCD K-factors decrease from 1.5 to 1.2, while the EW K-factors decrease from 0.95 to 0.4 for the p_{T} range of 200–2000 GeV. Pileup events are simulated and added to the hard scattering event. For each data-taking year the simulated events are weighted so that the number of pileup events matches the rate observed in the data.

JHEP08(2026)049

Events from the standard model processes $Z(\ell^+\ell^-)\gamma$, γ+jets, $\gamma\gamma$, $t\bar{t}\gamma$, and $t\gamma$ are produced at NLO in QCD using MadGraph5_aMC@NLO. Other background processes: WW, WZ, ZZ, $W(\mu\bar{\nu}_\mu)$, and $W(\tau\bar{\nu}_\tau)$ that have a very small contribution in the analysis were generated at LO with PYTHIA 8.

5 Photon identification

A dedicated high-p_T photon identifier (ID) [45] is used to distinguish high-p_T photons from jets. It uses a combination of the output of a boosted decision tree (BDT) and selections on the shower shape variables and the p_T and $|\eta|$ of the photon. The ID was trained using simulated events with high-p_T photons and with a simulated QCD sample to model the background that was generated with MadGraph5_aMC@NLO. Photons are identified by their BDT score and selections on three additional variables, which are the ratio of energies in the HCAL to the ECAL, the degree of isolation in the ECAL, and the degree of isolation in the tracker, determined after corrections for pileup and clustering inefficiencies have been applied. The efficiency of the ID for photons between 200 and 2000 GeV is estimated to be $(92 \pm 1)\%$, where the uncertainty is estimated from the variation of efficiency with p_T. This photon ID has a higher efficiency for photons with p_T greater than 200 GeV and a lower fake rate than the standard photon ID used in CMS, which is optimized for lower values of p_T [23]. Corrections applied as scale factors to account for the mismodeling of the identification efficiency are derived as functions of η and p_T using the tag-and-probe technique with $Z \to e^+e^-$ events, where the electrons are reconstructed as photons. The differences between the efficiencies found in data and simulation are typically less than 4%, with none greater than 10%.

6 Event selection

The trigger system selected candidate events where the p_T of the photon (p_T^γ) was above a threshold of 175 GeV in 2016, and 200 GeV in 2017 and 2018. This change was due to an increase in the instantaneous luminosity after 2016 requiring the trigger threshold to be raised to maintain the trigger rate within the bandwidth limits. In addition to the requirement on p_T^γ, the ratio between the energy deposited in the HCAL and in the ECAL associated with the photon candidate was required to be less than 0.15 for photons in the EB and less than 0.1 for photons in the EE.

During the 2016 and 2017 data-taking there was a gradual shift in the timing of the inputs of the ECAL L1 trigger in the region $2.5 < |\eta| < 3.0$ causing the trigger to be inefficient. For events containing a photon or an electron with $p_T > 50$ GeV, or a jet with $p_T > 100$ GeV in this region, there was an efficiency loss of $\approx$10–20%, depending on p_T, η, and when the data were taken. This resulted in a reduction of $\approx$2% in the number of events used in the analysis, correction factors for this effect were computed from data and applied to the event acceptance.

Signal events are required to have $p_T^{miss} > 200$ GeV and one photon with $p_T^\gamma > 225$ GeV, to be well above the trigger p_T threshold. The $|\eta^\gamma|$ of the photon candidate is required not to be between 1.44 and 1.57 [23] to avoid the region between the EB and the EE, and to have no more than one associated hit in the pixel detector [23].

To suppress beam-halo muons that can mimic high-p_{T} photons when they traverse the EB, the requirement $\mathrm{MIP_{tot}} < 4.9\,\mathrm{GeV}$ is applied to photons detected in the EB, where $\mathrm{MIP_{tot}}$ is the maximum of the total calorimeter energy summed along all possible paths of beam-halo that pass through the cluster.

Signals from spikes are suppressed using the method described in ref. [35]. To further suppress this background additional requirements are applied to the events. These are that the signal in the ECAL is within 3 ns of the bunch crossing time, and that the ratio of energy of the seed crystal to the higher of two neighboring crystals in the η direction is > 0.01.

To remove events with a misreconstructed $p_{\mathrm{T}}^{\mathrm{miss}}$ due to the jet energy resolution, events are discarded where at least one jet has a transverse momentum greater than 30 GeV and the angle $\Delta\phi$ between the jet and $\vec{p}_{\mathrm{T}}^{\mathrm{miss}}$ is less than 0.5. Events are also required to have $p_{\mathrm{T}}^{\gamma}/p_{\mathrm{T}}^{\mathrm{miss}}$ less than 1.4 to reject γ+jet background events. The value of 1.4 was selected to optimize the suppression of background events, in particular those from γ + jet events. These two criteria remove more than 99% of the γ+jet background events. The selected photon and the missing transverse momentum are also required to be separated in azimuthal angle $\Delta\phi(p_{\mathrm{T}}^{\gamma}, p_{\mathrm{T}}^{\mathrm{miss}}) > 2.0$ to suppress $\mathrm{W}(\mathrm{e}\overline{\nu}_{\mathrm{e}})$ events where the electron has one, or no hits in the pixel detector.

During the 2018 data taking, two modules of the HCAL were inoperable, affecting the jet identification and jet energy measurement in the region $-1.57 < \phi < -0.87$ and $-3.0 < \eta < -1.3$. Events with a jet with $p_{\mathrm{T}}^{\mathrm{jet}} > 15\,\mathrm{GeV}$ in this region are excluded. The selected photon candidate is also required to be outside of this region to suppress backgrounds from jets misidentified as photons. To suppress background events from $W(\ell\overline{\nu}_{\ell})\gamma$ processes, events with an electron or a muon with $p_{\mathrm{T}} > 10\,\mathrm{GeV}$ and passing loose identification criteria [23, 46] are also discarded. Table 1 summarizes the principal selections used in the signal region (SR).

Two control regions, $\mathrm{CR_e}$ and CR_{μ}, are used to estimate the $W(\ell\overline{\nu}_{\ell})\gamma$ background. Events in these CRs are required to have an electron or a muon candidate, identified with tight criteria, with $p_{\mathrm{T}} > 30\,\mathrm{GeV}$, a photon satisfying the same signal requirements as in the SR, and the transverse mass of the $p_{\mathrm{T}}^{\mathrm{miss}} + \ell$ system less than 160 GeV. For these events the vector sum $\vec{R}_{\mathrm{T}} = \vec{p}_{\mathrm{T}}^{\mathrm{miss}} + \vec{p}_{\mathrm{T}}^{\,\ell}$ is a proxy for the $\vec{p}_{\mathrm{T}}^{\mathrm{miss}}$ in the SR, and the same requirements applied on $\vec{p}_{\mathrm{T}}^{\mathrm{miss}}$ in the SR are applied on R_{T}. The selections applied in the SR to account for the inoperable HCAL modules in 2018 are applied with the additional requirement that the lepton is not in this region. Events are not included in the CRs if they contain a jet that has a $p_{\mathrm{T}}^{\mathrm{jet}} > 30\,\mathrm{GeV}$ and an angular separation from $\vec{p}_{\mathrm{T}}^{\mathrm{miss}}$, $\Delta\phi(\mathrm{jet}, \vec{p}_{\mathrm{T}}^{\mathrm{miss}}) < 0.5$. We also only include leptons that have $\Delta R = \sqrt{(\Delta\eta)^2 + (\Delta\phi)^2}$ between the lepton and the jet greater than 0.5. Additionally, the lepton and the photon must be separated by $\Delta R(\mathrm{e}, \gamma) > 0.5$.

JHEP08(2026)049

Events are selected if the event contains:
Exactly one photon with $p_T^{\gamma} > 225\,\text{GeV}$, with
$H/E < 0.15(0.1)$ EB, (EE); $(\lvert\eta^{\gamma}\rvert < 1.44) \cup (1.57 < \lvert\eta^{\gamma}\rvert < 2.5)$;
$p_{\mathrm{T}}^{\text{miss}} > 200\,\text{GeV}$; $p_T^{\gamma}/p_{\mathrm{T}}^{\text{miss}} < 1.4$, and $\Delta\phi(\vec{p}_{\mathrm{T}}^{\text{miss}}, \gamma) > 2$.
Events are not selected if the event contains:
a jet with $p_{\mathrm{T}}^{\text{jet}} > 30\,\text{GeV}$ and $\Delta\phi(\text{jet}, \vec{p}_{\mathrm{T}}^{\text{miss}}) < 0.5$,
or a muon with $p_{\mathrm{T}}^{\mu} > 10\,\text{GeV}$,
or an electron with $p_{\mathrm{T}}^{\mathrm{e}} > 10\,\text{GeV}$ and $\Delta R(\mathrm{e}, \gamma) > 0.1$.

Table 1. Principal signal event selection criteria. Further details of the event selection, including fiducial criteria, are provided in the text.

7 Background estimation

7.1 Jets misidentified as photons

Electromagnetic deposits in the ECAL produced by jets with few tracks and a small signal in the HCAL can be misidentified as photons, and, when associated with a high $p_{\mathrm{T}}^{\text{miss}}$ are a background to the $\mathrm{Z}(\nu\bar{\nu})\gamma$ signal. This background, which comes mainly from the $\mathrm{Z}(\nu\bar{\nu})$+jets process and from events with multiple jets, is estimated by first computing the probability of misidentifying a jet in events with $p_{\mathrm{T}}^{\text{miss}} < 40\,\text{GeV}$. For this, photon-like objects from the electromagnetic deposits of a jet were selected by inverting the isolation selection criteria. The misidentification ratio is then defined as the ratio of the observed number of photons that pass the photon ID to the number that pass less stringent photon ID requirements.

Since the numerator can still be contaminated with genuine photons, we estimate this contamination by fitting the BDT score distribution in data to a combination of two templates, one for genuine photons and another for misidentified photons. The template for genuine photons is obtained from simulated $\mathrm{pp} \to \gamma$+jets events and the one for misidentified photons is obtained directly from a data sideband, chosen by requiring the photon to have a large number of tracks within the photon's isolation cone.

The misidentification ratio is then estimated in bins of p_{T}^{γ} for the EB and EE separately. It is then applied to a sample of events in data with photon candidates that have passed the same less stringent criteria used for the denominator of the misidentification ratio to estimate the contribution of jets misidentified as photons in the SR.

The sources of uncertainty in the estimate of this background are the definition of the background templates, the criteria on the $p_{\mathrm{T}}^{\text{miss}}$ for the ratio estimation, the modeling of the BDT variable for genuine photons in simulation, and the binning and statistical uncertainties of the simulated signal photons in the template fitting. How these are taken into account is discussed in section 9.

7.2 Electrons misidentified as photons

Standard model processes, such as $\mathrm{W(e\overline{\nu}_e)}$ and $\mathrm{W(e\overline{\nu}_e)Z(\nu\overline{\nu})}$ production, can mimic the $\mathrm{Z(\nu\overline{\nu})\gamma}$ signature when the electron is reconstructed as a photon, which occurs when one or more layer of the pixel detector does not detect the electron. The estimate of the electron-to-photon misidentification ratio is made with $\mathrm{Z \to e^+e^-}$ events using the tag-and-probe method [23], with the electron tag required to have $p_{\mathrm{T}} > 20\,\mathrm{GeV}$ and the probe to have $p_{\mathrm{T}} > 200\,\mathrm{GeV}$. The invariant mass of the tag-probe pair is required to be between 60 and 120 GeV and a passing (failing) probe is then defined if the electron is (is not) reconstructed as an electron candidate [23]. The passing and failing probes are fit simultaneously with a signal plus background model. The invariant mass shape of the signal is obtained from simulation and the background shape is parameterized using an exponential function.

Since the pixel detector efficiency is $|\eta|$-dependent, the misidentification ratio is evaluated in bins of $|\eta|$. For electrons detected in the EB, three bins are used: 0.0–0.6, 0.6–1.1, 1.1–1.44, with the estimated ratio across the three years ranging from 0.01 in the highest $|\eta|$ region to 0.045 in the lowest $|\eta|$ region. In the EE only a single $|\eta|$ range covering 1.57 to 2.5 is used due to the low number of high-p_{T} electrons detected, and the ratio is estimated to be between 0.0058–0.0165 for the three years. Additionally, the efficiencies of certain parts of the pixel detector changed during the three years of data taking; for these regions separate misidentification ratios determined for each year are used.

The sources of uncertainty for the treatment of this background mainly arise from the limited number of events that fail the probe criteria, which varies across the different η regions, and the choice of the signal and background models.

7.3 Background due to $\mathrm{W(\ell\nu_\ell)\gamma}$

The $\mathrm{W(\ell\nu_\ell)\gamma}$ process contributes to the background when the W boson decays leptonically and the charged lepton ℓ is undetected due to acceptance limitations or reconstruction failure. This background is estimated via a simultaneous likelihood fit to data from the SR and to the two control regions, $\mathrm{CR_e}$ and $\mathrm{CR_\mu}$, which are kinematically similar to the SR but enriched in $\mathrm{W(\ell\nu_\ell)\gamma}$ events by requiring an electron or a muon. These control regions provide a direct constraint on the $\mathrm{W(\ell\nu_\ell)\gamma}$ background normalization, reducing reliance on theoretical cross-section predictions. All $p_{\mathrm{T}}^{\mathrm{miss}}$-related criteria from the SR are transferred to the transverse recoil momentum, $\vec{R}_T$, ensuring phase space consistency.

Events are not added to the CRs if the lepton is collinear with an energetic jet, so as to exclude events with final-state radiation. Events from 2018 where the lepton is in one of the inoperable HCAL regions are also not included.

The expected $W(\ell\overline{\nu}_\ell)\gamma$ contribution is initially modeled using simulation, with the p_{T} distribution corrected for next-to-next-to-leading order (NNLO) QCD [41] and next-to-leading order (NLO) electroweak [43] effects. Free parameters for each p_{T} bin are used to scale the process yield uniformly across all three regions. In the simultaneous fit, the SR-to-CR yield ratios are fixed for each bin, while the overall normalization is set with the data.

7.4 Other backgrounds

Other background sources include the spike signals in the APDs, which can be misidentified as high-p_{T} photons with a large $p_{\mathrm{T}}^{\mathrm{miss}}$, and bremsstrahlung radiation from beam-halo muons in the ECAL detector that can produce a photon-like signature in both EB and EE.

To estimate the number of spike signals within the 3 ns event window, the distribution of the arrival time of the photon events is fit with signal and background timing distribution templates. The background template is derived from spikes and beam-halo events. The timing distribution of spikes is derived from a dedicated control region in data, selecting photons with large signals in the central crystals and small signals in the adjacent crystals. The beam-halo template is derived by selecting photons with large $\mathrm{MIP_{tot}}$ values, and the signal template is obtained from $\mathrm{Z} \to \mathrm{e^+e^-}$ events in data.

The estimated number of spikes obtained from this fit ranges from 9.4 to 20.8 across the three years of data-taking, with an uncertainty no more than 17%, while the contribution from beam-halo to the total estimated background is negligible. A more detailed description of the spike background estimation procedure can be found in ref. [47].

In the EE, the background due to bremsstrahlung radiation by beam-halo muons is the predominant source of background and the strategy used in the EB to remove this background is ineffective in the EE due to its geometry. In this region, beam-halo muons cross the EE nearly parallel to the beamline and the bremsstrahlung photons that they produce deposit energy in a small number of adjacent crystals making them difficult to distinguish from photons produced at the interaction point. To suppress this background the score of a dedicated BDT using the angle between a line joining the hits in the EE, and either the HCAL endcap or the ES, and the beam line, and the energy deposited in both the HE and ES, as well as the ECAL shower shape variables are used to separate signal from beam-halo events. The application of this BDT reduces the beam-halo background to <0.2% of its initial contribution in all the 3 years.

The remaining contribution of the beam halo to the total background is evaluated by fitting the ϕ distribution with the signal template, obtained from simulation, and a background template, extracted from data by inverting the BDT tagger requirement.

8 Systematic uncertainties

For simulated signal and background sources, uncertainties are assigned to the estimated luminosity of the dataset, the efficiencies of the trigger and photon identification, the calibration of the jet energy scale and resolution, the calibration of the photon energy scale and resolution, and the modeling of the pileup interactions. In addition, uncertainties are assigned for the choice of PDF set and for the missing higher orders in QCD calculations by varying of the renormalization and factorization scales, μ_{R} and μ_{F}. These uncertainties can affect the shape of the p_T^{γ} spectrum and the event yield. The large uncertainties in the background due to electrons misidentified as photons, and jets misidentified as photons are due to the limited number of events in the control regions where the misidentification ratio is measured.

JHEP08(2026)049

The uncertainties in the integrated luminosity are estimated to be 1.3% (2016), 2.2% (2017), and 2.5% (2018) [48–50]. In addition, the total integrated luminosity has an uncertainty of 1.6% reflecting the uncorrelated time evolution of some systematic effects. Simulated background events are weighted in order to match the expected pileup distribution obtained using the inelastic pp interaction cross section, $69.2 \pm 4.6\,\mathrm{mb}$ [51].

The uncertainties in the correction factors that account for the difference in the lepton ID efficiencies between data and simulated data are below 0.01%. An uncertainty of between 3.5% and 4.7% is assigned to the correction factors, to account for the difference between the photon ID efficiencies in data and simulated data.

To assess the impact of the uncertainties in the photon energy scale and resolution the electron and photon energies are varied by around 0.1 (0.3)% in the EB (EE) [23]. As the signal photon is required to not have a pixel detector seed in the tracker, the uncertainty due to mismodeling of the efficiency of this requirement is obtained in the data and is under 0.9%.

Jet p_T measurement uncertainties are propagated by varying the energy corrections within their estimated uncertainties. This affects the yields due to the phase space selection on $\Delta\phi_{\min}(\vec{p}_{\mathrm{T}}^{\,\mathrm{jet}}, \vec{p}_{\mathrm{T}}^{\,\mathrm{miss}})$ in the SR and $\Delta\phi_{\min}(\vec{p}_{\mathrm{T}}^{\,\mathrm{jet}}, \vec{R}_{\mathrm{T}})$ in the CRs, where only jets with p_{T} larger than 30 GeV are considered. The jet energy variations and the corresponding $\vec{p}_{\mathrm{T}}^{\,\mathrm{miss}}$ variations are correlated and are thus found simultaneously in the calculations of the yields. The L1 ECAL trigger inefficiency due to timing misalignment [20] is not included in the simulation; weights to correct for this are extracted from data. The uncertainty associated with these weights is about 1.3% for 2016 and 1.9% for 2017 and 2018. The uncertainty in the $\mathrm{e} \to \gamma$ misidentification ratio and the jet $\to \gamma$ misidentification, described in sections 7.2 and 7.1, ranges from 4% to 20%.

Uncertainties in the NNLO QCD corrections for $\mathrm{Z}(\nu\bar{\nu})\gamma$ production are assigned for the μ_{F} and μ_{R} scales calculated with MATRIX [52], and for shape variations following the prescription in ref. [53]. Uncertainties in NLO electroweak corrections are assigned as prescribed in refs. [42, 43]. The simulated background estimates use the NNPDF 3.1 Hessian PDF set. The uncertainties due to PDF and α_{S} are estimated following the PDF4LHC recipe [54]. The uncertainties due to missing higher QCD orders, which includes the renormalization and factorization scale choice, and QCD NNLO corrections, are estimated by independently varying the two scales by factors of 0.5 and 2 with the constraint $0.5 \leq \mu_{\mathrm{R}}/\mu_{\mathrm{F}} \leq 2$, and taking the envelope (max and min) of the 7-point variations. The values of these systematic uncertainties are given in table 2. The uncertainties of the photon ID corrections and the jet energy scale are the two leading sources of systematic uncertainty in this analysis.

9 Statistical analysis

Cross section measurements and the constraints on the anomalous coupling parameters are evaluated by constructing a binned profile likelihood function to determine the best fit parameters to the data using the COMBINE tool of CMS [55]. The binned likelihood

JHEP08(2026)049

Source		Correlated between years
	Experimental	
Integrated luminosity	1.3–2.5%	Partially
Pileup	0.4–2.2%	✓
Lepton ID corrections	< 0.01%	✓
Photon ID corrections	3.5–4.7%	✓
Photon energy scale and resolution	0.2–1.1 %	✓
Photon pixel veto corrections	0.1–0.9%	✓
Jet energy scale and resolution	0.2–2.8%	Partially
L1 ECAL inefficiency	0.1–1.9%	✓
Jet$\rightarrow\gamma$ misid. ratio	2–20%	✓
e $\rightarrow\gamma$ misid. ratio	13–45%	✓
	Theoretical	
NLO EW corrections	2.7%	✓
PDF and α_S	1.5-1.7%	✓
Renormalization and factorization scale	6–7.2%	✓

Table 2. Sources of systematic uncertainties and their estimated contributions. The ✓ symbol indicates full correlation between the data-taking years.

function is defined as:

$$\begin{aligned}\mathcal{L}(\vec{d}\mid\vec{\mu},\vec{r}^{\mathrm{W}\gamma},\vec{\theta}) = \prod_i\Big[&\mathcal{P}\big(d_i|s_i(\vec{\mu},\vec{\theta}) + r_i^{\mathrm{W}\gamma}\,N_i^{\mathrm{SR,\,W}\gamma}(\vec{\theta}) + b_i(\vec{\theta})\big)\\ &\times\prod_{K=\mathrm{e},\mu}\mathcal{P}\big(d_i^K|r_i^{\mathrm{W}\gamma}\,N_i^{K,\,\mathrm{W}\gamma}(\vec{\theta}) + b_i^K(\vec{\theta})\big)\Big]\\ &\times\prod_j\mathcal{N}(\theta_j),\end{aligned} \tag{9.1}$$

where i denotes the index for the p_{T}^{γ}-bins, $\vec{\mu}$ represents the parameters of interest, which are either the aNTGC coupling parameters (h_3 and h_4) or the cross sections, while $\vec{\theta}$ denotes the nuisance parameters associated with systematic uncertainties. The uncertainties due to limited statistics of the simulated samples are incorporated using Barlow-Beeston Lite method [56]. The symbol $\mathcal{P}$ indicates the Poisson distribution and $\mathcal{N}$ the normal distribution. Within bin i, the observed event counts in the SR and CR_K (indexed by $K = \mathrm{e},\mu$) are denoted by d_i and d_i^K, respectively. The contributions from the $\mathrm{W}(\ell\nu_\ell)\gamma$ process, estimated by simulation, are $N_i^{\mathrm{SR,W}\gamma}$ and $N_i^{K,\mathrm{W}\gamma}$, while the contributions from all other background processes are b_i and b_i^K in the SR and CR_K, respectively. A free parameter, $r_i^{W\ \gamma}$, scales the simulated estimates of the $\mathrm{W}(\ell\nu_\ell)\gamma$ process within each bin i in all three regions, thereby constraining the rate of this background. The signal terms s_i are defined in terms of the parameters of interest, which are extracted by a simultaneous maximum likelihood fit to the data. Table 3 shows the post-fit event yields in the photon-p_{T} spectrum for the combined phase space extracted after a simultaneous fit to the data in the signal and control regions.

JHEP08(2026)049

Predicted	Barrel	Endcaps
Fiducial Zγ	1456 ± 73	305 ± 17
Non-fiducial Zγ	72.2 ± 9.8	21.8 ± 2.9
$e \to \gamma$	404 ± 53	37.4 ± 11.1
$W(\ell\nu_\ell)\gamma$	319 ± 29	69.8 ± 8.1
jet $\to \gamma$	34.5 ± 0.8	12.2 ± 0.6
Minor backgrounds	153 ± 28	81 ± 89
Spikes	40.3 ± 3.7	—
Beam halo	—	9.5 ± 0.5
Total Predicted	2480 ± 51	539 ± 184
Observed	2453	568

Table 3. Post-fit event yields in the photon-p_T spectrum for the combined phase space. These numbers are extracted after a simultaneous fit to the data in the signal and control regions. The "others" background include contributions from nonfiducial $Z(\nu\bar{\nu})\gamma$, $Z/\gamma^*(\ell^+\ell^-)\gamma$, $t\bar{t}\gamma$, $WV\gamma$, single-t+γ, VV, single-W, and jet misidentified as a photon.

As expected, due to the high-p_T of the photon, the EB has significantly more events than the EE. Separately, as a confirmation, in a fit to only the control regions the estimated number of $W(\ell\nu_\ell)\gamma$ events in the signal region is 321 ± 19 in the barrel region and 69.8 ± 6.3 in the endcap region, which is consistent with the yields obtained in the simultaneous fit.

10 Results

10.1 Fiducial cross section and differential cross section

The inclusive differential cross section for the $Z(\nu\bar{\nu})\gamma$ process is measured with a likelihood-based unfolding technique [57] that accounts for the impact of the detector acceptance, efficiency, and resolution. The measurements correspond to a fiducial region at the generator level of the particles before any interaction with the detector. This region is defined by criteria that closely match the detector level phase space of the SR. The selections applied on the generator level variables of the simulated signal are:

- $(|\eta^\gamma| < 1.44) \cup (1.57 < |\eta^\gamma| < 2.5)$,
- $p_T^\gamma > 225\,\text{GeV}$,
- $p_T^{\text{miss}} > 200\,\text{GeV}$,
- $\frac{p_T^\gamma}{p_T^{\text{miss}}} < 1.4$,
- $\Delta\phi(\vec{p}_T^{\text{miss}}, \gamma) > 2$,

where $\vec{p}_T^{\text{miss}}$ is the magnitude of the vector sum $\vec{p}_T$ of the two neutrinos coming from the Z boson at the generator level, and $\Delta\phi(\vec{p}_T^{\text{miss}}, \gamma)$ refers to the azimuthal angle between the transverse momentum vector of the generator-level photon and $\vec{p}_T^{\text{miss}}$.

We construct the response matrix, R_{ij}, which models the detector response to the events produced in the fiducial region to quantify the probability with which an event produced with a generator level photon p_T in bin j will be observed with detector-level photon p_T in bin i. This is used to account for bin migration due to the detector energy resolution, efficiency and acceptance. We calculate the number of events from the signal simulation, N_{ij}^{detector}, in the detector-level bin i that are actually produced in the generator level bin j. The sample also provides the total number of generator level fiducial events, $N_j^{\text{generator}}$, produced in the generator level bin j. The response matrix is then defined as:

$$R_{ij} = \frac{N_{ij}^{\text{detector}}}{N_j^{\text{generator}}}. \tag{10.1}$$

This response is used to model the signal, s_i, within the likelihood function as given in section 9. The number of expected signal events in detector bin i is expressed as a sum of contributions from the generator level bins j, each associated with unknown cross sections σ_j. Additionally, there is a minor contribution, $s_i^{\text{nonfiducial}}$, originating from signal process events occurring outside of the fiducial region. These nonfiducial events are treated as background in this measurement. The full signal model is:

$$s_i = s_i^{\text{nonfiducial}} + \sum_j \mathcal{L}\, \sigma_j\, R_{ij}, \tag{10.2}$$

where $\mathcal{L}$ is the integrated luminosity. The value of $\mathcal{L}\,\sigma_j$ is the true number of events produced at the generator level in bin j, which is reduced by the detector response R_{ij} in the sum. The terms $\{\sigma_j\}$ are treated as free parameters and obtained from a maximum likelihood fit to derive the differential cross sections. The chosen bin boundaries for the photon's generator level p_T are: 225, 275, 350, 450, 600, 800, and 1500 GeV.

The measured cross-sections and the predictions at NLO and NNLO in QCD using MadGraph5_aMC@NLO [37] and MATRIX [52] are shown in table 4. Due to nuisance parameters being pulled to different values in different fit configurations, the sum of the cross section in the EB and EE is not exactly equal to the combined cross section. Figure 4 shows the observed and fitted distributions of photon p_T in the barrel and endcap regions of the phase space obtained separately after performing the fit for the measurement of the differential cross sections for the combined phase space. For these distributions, the $W(\ell\nu_\ell)\gamma$ background is estimated only from the control region fit.

The measured differential cross sections and the theoretical predictions of MadGraph5_aMC@NLO and MATRIX as a function of p_T^γ are shown in figure 5 and are listed in table 5. The theoretical predictions have uncertainties from renormalization and factorization scale variation, as well as numerical precision. Additionally, MadGraph5_aMC@NLO includes the uncertainties of parton density functions. While the theoretical predictions are all higher than the measured cross-sections, the differences are all within the uncertainties, except for the p_T bins 275–350 GeV and 350–450 GeV, where the differences are $\approx 2\sigma$, with the NNLO(MATRIX) predictions in better agreement than those from MadGraph5_aMC@NLO. The low p_T bins have the highest correlation where it ranges between 0.20 and 0.27. The binning in detector-level photon p_T is optimized using the Bayesian Block algorithm [58].

JHEP08(2026)049

Region	Measured	NLO (MadGraph5_aMC@NLO)	NNLO (MATRIX)
Barrel $\lvert\eta\rvert < 1.4442$	$16.7^{+1.0}_{-1.0}$	$19.6^{+0.7}_{-0.7}$	$19.3^{+0.3}_{-0.3}$
Endcaps $1.566 < \lvert\eta\rvert < 2.5$	$7.8^{+0.8}_{-0.7}$	$6.4^{+0.3}_{-0.3}$	$6.21^{+0.07}_{-0.09}$
Total	$23.3^{+1.4}_{-1.3}$	$26.1^{+1.0}_{-1.0}$	$25.4^{+0.4}_{-0.3}$

Table 4. Measured and predicted cross sections in femtobarns evaluated in the barrel, the endcaps, and the combined fiducial phase space. The predicted cross sections are calculated at NLO and NNLO in QCD. Due to nuisance parameters being pulled to different values in different fit configurations, the sum of the cross section in the EB and EE is not exactly equal to the combined cross section.

p_{T}-range (GeV)	Measured	NLO (MadGraph5_aMC@NLO)	NNLO (MATRIX)
225–275	$12.45^{+0.91}_{-0.87}$	$12.88^{+0.42}_{-0.49}$	$12.83^{+0.17}_{-0.15}$
275–350	$6.95^{+0.60}_{-0.57}$	$8.14^{+0.31}_{-0.30}$	$7.89^{+0.16}_{-0.15}$
350–450	$2.61^{+0.35}_{-0.33}$	$3.34^{+0.17}_{-0.11}$	$3.22^{+0.07}_{-0.06}$
450–600	$1.08^{+0.21}_{-0.20}$	$1.26^{+0.08}_{-0.05}$	$1.22^{+0.02}_{-0.02}$
600–800	$0.282^{+0.010}_{-0.009}$	$0.345^{+0.026}_{-0.019}$	$0.331^{+0.007}_{-0.005}$
800–1500	$0.092^{+0.005}_{-0.005}$	$0.107^{+0.011}_{-0.012}$	$0.091^{+0.020}_{-0.014}$

Table 5. Measured and predicted cross sections in femtobarns in bins of p_{T}^{γ}.

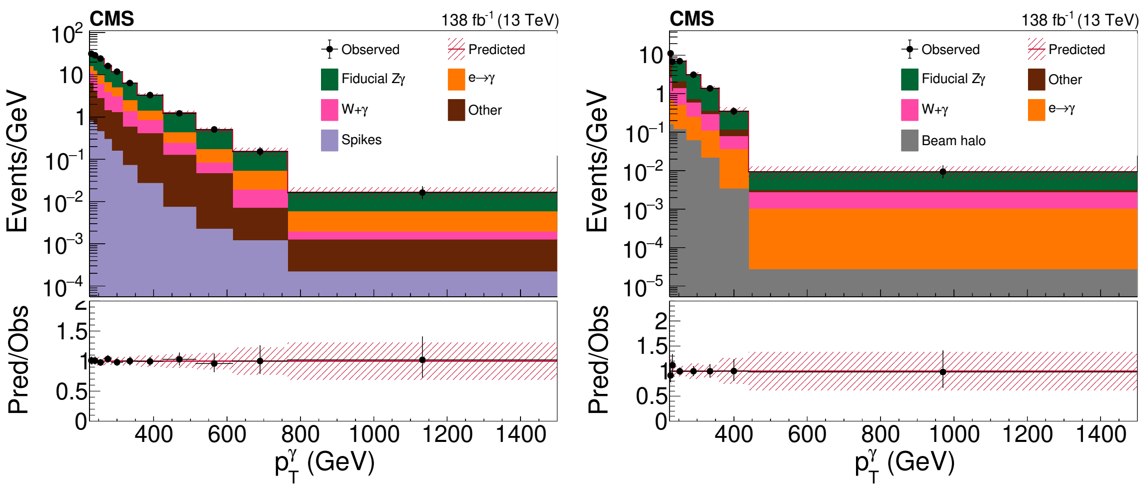

Figure 4. The post-fit reconstruction-level distributions in the signal region after the combined (barrel+endcap) differential cross section fit (left: barrel region, right: endcap region). The Predicted distribution is the full model with all parameters fixed to their post-fit values. Note in particular that the free cross section parameters for the signal are also fixed to their post-fit values and then propagated through the response matrix. The bars on the black data points indicate the statistical uncertainty in the data, while the red band shows the total post-fit model uncertainty.

JHEP08(2026)049

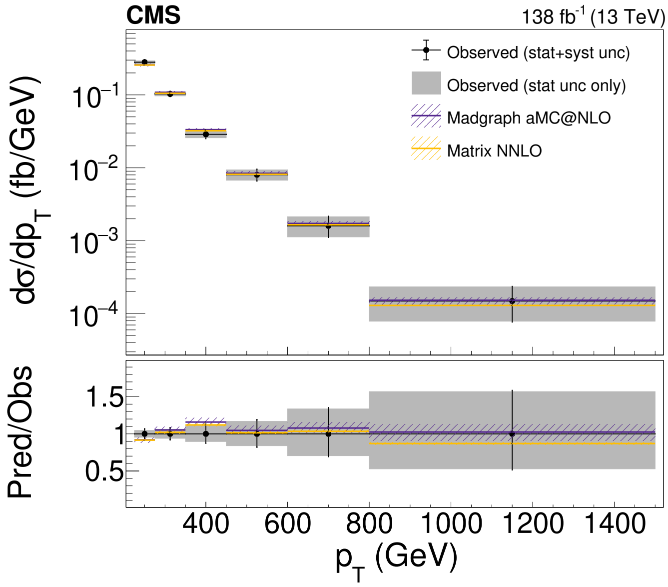

Figure 5. Measured and predicted differential cross sections as function of p_T^γ for the combined fiducial phase space. The colored bands associated with the predictions indicate the theoretical uncertainties associated with the MadGraph5_aMC@NLO and MATRIX generators. For the measured cross sections, the grey band indicates the statistical uncertainty of the fit, while the error bars on the black data points indicate the total uncertainty of the fit, including both statistical and systematic components.

10.2 Limits on anomalous couplings

We parameterize the aNTGC prediction for the SR by fitting the simulated yields to different pairs of coupling values with a two-dimensional quadratic function of h_3^Z and h_4^Z as a function of p_T^γ. This parameterization is then used to fit the likelihood simultaneously in the EB and the EE. To calculate the likelihoods, the binning chosen is the same as that used for the histograms in figure 4. The coefficients of the parameterization are varied to determine the systematic uncertainties. The confidence contours obtained are shown in figure 6. As the interference term in the Lagrangian becomes negligible at high transverse momentum, the measurement is insensitive to the sign of the couplings, we therefore quote the best fit points in the data at the local minima. In addition, one-dimensional confidence intervals for each parameter, with the other parameters fixed at zero, are shown in table 6. In figure 7, the predicted p_T^γ distribution after performing the fit under the SM-only hypothesis is compared with the predictions at the upper boundaries of the observed 1D confidence intervals of the coupling parameters.

11 Summary

We have measured the inclusive and differential cross sections of $Z(\nu\bar{\nu})\gamma$ in proton-proton collisions at $\sqrt{s} = 13\,\text{TeV}$ using data collected with the CMS detector between 2016 and 2018, corresponding to an integrated luminosity of $138\,\text{fb}^{-1}$. The fiducial $Z\gamma$ cross section, where a photon with a p_T greater than $225\,\text{GeV}$ is produced in association with a Z, and the Z decays

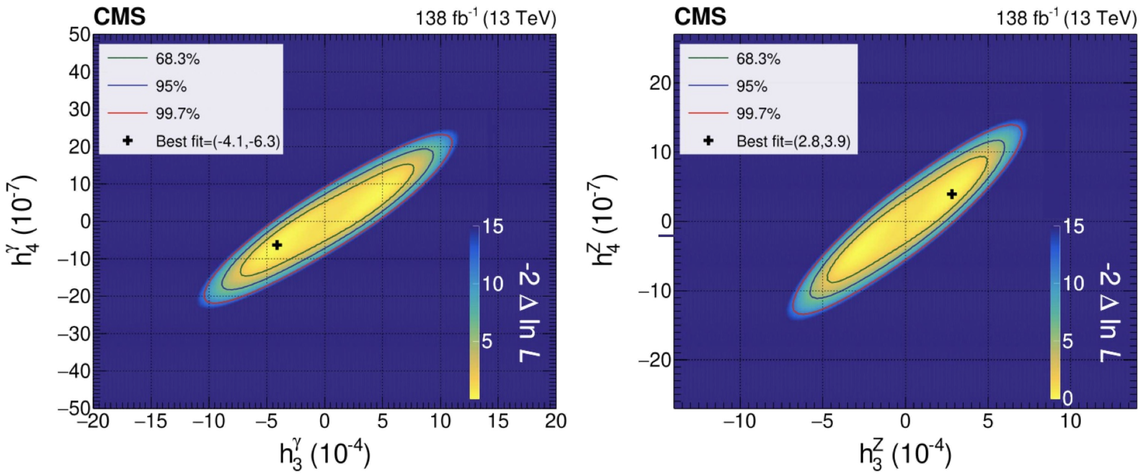

Figure 6. Confidence contours of the aNTGC parameters h_3^γ, h_4^γ (left) and h_3^Z, h_4^Z (right) with the best fit points, which are the local minima of the negative log likelihood.

Parameter	Expected	Observed
$h_3^\gamma \times 10^4$	$(-2.8,\ 2.9)$	$(-3.4,\ 3.5)$
$h_4^\gamma \times 10^7$	$(-5.9,\ 6.0)$	$(-6.8,\ 6.8)$
$h_3^Z \times 10^4$	$(-1.8,1.9)$	$(-2.2,\ 2.2)$
$h_4^Z \times 10^7$	$(-3.7,\ 3.7)$	$(-4.1,\ 4.2)$

Table 6. Expected and observed 95% confidence level intervals of the parameters of anomalous couplings (with the other parameters fixed at zero).

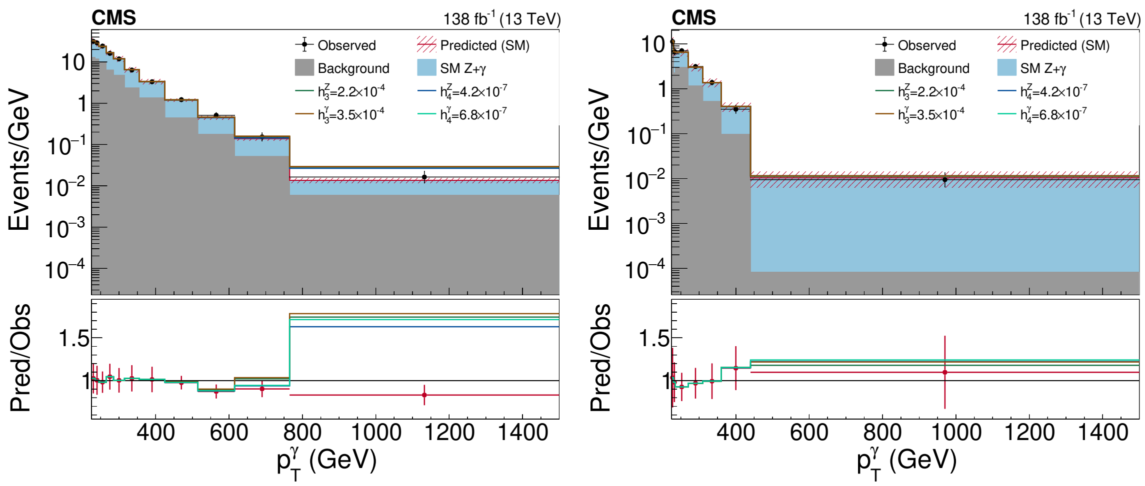

Figure 7. Comparison of the predicted distribution of p_T^γ under the SM-only hypothesis in the barrel (left), and in the endcaps (right) phase space with the predictions at the upper boundaries of the observed 1D confidence intervals of the coupling parameters. The lower panels compare the SM (shown in red) and the aNTGC predictions, with the observed p_T^γ distribution (shown in black). The uncertainties on the data are statistical only; the uncertainties on SM predictions include renormalization and factorization scale variations.

JHEP08(2026)049

to a $\nu\bar{\nu}$ pair ($Z(\nu\bar{\nu})\gamma$), is measured to be $23.3^{+1.4}_{-1.3}$ fb, in agreement, within uncertainties, with the standard model prediction, which are $26.07^{+0.96}_{-0.97}$ fb from MadGraph5_aMC@NLO and $25.45^{+0.41}_{-0.33}$ fb from MATRIX (NNLO). The differential $Z(\nu\bar{\nu})\gamma$ cross section as function of photon transverse momentum has been measured and compared with the standard model predictions computed at next-to-leading and next-to-next-to-leading orders in perturbative quantum chromodynamics. With these data we have probed the presence of anomalous couplings that affect the $ZZ\gamma$ vertex by using the p_T spectrum of the photons as the sensitive variable. No evidence is found for anomalous neutral trilinear gauge couplings in $Z\gamma$ production. The observed 95% confidence level intervals for h_3^γ and h_4^γ are determined to be $(-3.4, 3.5)\times10^{-4}$ and $(-6.8, 6.8)\times10^{-7}$; and for h_3^Z and h_4^Z $(-2.2, 2.2)\times10^{-4}$ and $(-4.1, 4.2)\times10^{-7}$, respectively. These are stricter than the earlier limits on h_3^γ, h_3^Z, and h_4^Z.

Acknowledgments

We congratulate our colleagues in the CERN accelerator departments for the excellent performance of the LHC and thank the technical and administrative staffs at CERN and at other CMS institutes for their contributions to the success of the CMS effort. In addition, we gratefully acknowledge the computing centers and personnel of the Worldwide LHC Computing Grid and other centers for delivering so effectively the computing infrastructure essential to our analyses. Finally, we acknowledge the enduring support for the construction and operation of the LHC, the CMS detector, and the supporting computing infrastructure provided by the following funding agencies: SC (Armenia), BMBWF and FWF (Austria); FNRS and FWO (Belgium); CNPq, CAPES, FAPERJ, FAPERGS, and FAPESP (Brazil); MES and BNSF (Bulgaria); CERN; CAS, MoST, and NSFC (China); MINCIENCIAS (Colombia); MSES and CSF (Croatia); RIF (Cyprus); SENESCYT (Ecuador); ERC PRG, TARISTU24-TK10 and MoER TK202 (Estonia); Academy of Finland, MEC, and HIP (Finland); CEA and CNRS/IN2P3 (France); SRNSF (Georgia); BMFTR, DFG, and HGF (Germany); GSRI (Greece); NKFIH (Hungary); DAE and DST (India); IPM (Iran); SFI (Ireland); INFN (Italy); MSIT and NRF (Republic of Korea); MES (Latvia); LMTLT (Lithuania); MOE and UM (Malaysia); BUAP, CINVESTAV, CONACYT, LNS, SEP, and UASLP-FAI (Mexico); MOS (Montenegro); MBIE (New Zealand); PAEC (Pakistan); MES, NSC, and NAWA (Poland); FCT (Portugal); MESTD (Serbia); MICIU/AEI and PCTI (Spain); MOSTR (Sri Lanka); Swiss Funding Agencies (Switzerland); MST (Taipei); MHESI (Thailand); TUBITAK and TENMAK (Türkiye); NASU (Ukraine); STFC (United Kingdom); DOE and NSF (U.S.A.).

Individuals have received support from the Marie-Curie program and the European Research Council and Horizon 2020 Grant, contract Nos. 675440, 724704, 752730, 758316, 765710, 824093, 101115353, 101002207, 101001205, and COST Action CA16108 (European Union); the Leventis Foundation; the Alfred P. Sloan Foundation; the Alexander von Humboldt Foundation; the Science Committee, project no. 22rl-037 (Armenia); the Fonds pour la Formation à la Recherche dans l'Industrie et dans l'Agriculture (FRIA) and Fonds voor Wetenschappelijk Onderzoek contract No. 1228724N (Belgium); the Beijing Municipal Science & Technology Commission, No. Z191100007219010, the Fundamental Research Funds for the Central Universities, the Ministry of Science and Technology of China under Grant No. 2023YFA1605804, the Natural Science Foundation of China under Grant No. 12535004, and USTC Research Funds of the Double First-Class Initiative No. YD2030002017 (China); the Ministry of Education, Youth and Sports (MEYS) of the Czech Republic; the Shota Rustaveli National Science Foundation, grant FR-22-985 (Georgia); the Deutsche Forschungsgemeinschaft (DFG), among others, under Germany's Excellence Strategy – EXC 2121 "Quantum Universe" – 390833306, and under project number 400140256 – GRK2497; the Hellenic Foundation for Research and Innovation (HFRI), Project Number 2288 (Greece); the Hungarian Academy of Sciences, the New National Excellence Program – ÚNKP, the NKFIH research grants K 131991, K 133046, K 138136, K 143460, K 143477, K 146913, K 146914, K 147048, 2020-2.2.1-ED-2021-00181, TKP2021-NKTA-64, and 2025-1.1.5-NEMZ_KI-2025-00004 (Hungary); the Council of Science and Industrial Research, India; ICSC – National Research Center for High Performance Computing, Big Data and Quantum Computing, FAIR – Future Artificial Intelligence Research, and CUP I53D23001070006 (Mission 4 Component 1), funded by the NextGenerationEU program (Italy); the Latvian Council of Science; the Ministry of Education and Science, project no. 2022/WK/14, and the National Science Center, contracts Opus 2021/41/B/ST2/01369, 2021/43/B/ST2/01552, 2023/49/B/ST2/03273, and the NAWA contract BPN/PPO/2021/1/00011 (Poland); the Fundação para a Ciência e a Tecnologia, grant CEECIND/01334/2018 (Portugal); the National Priorities Research Program by Qatar National Research Fund; MICIU/AEI/10.13039/501100011033, ERDF/EU, "European Union NextGenerationEU/PRTR", and Programa Severo Ochoa del Principado de Asturias (Spain); the Chulalongkorn Academic into Its 2nd Century Project Advancement Project, the National Science, Research and Innovation Fund program IND_FF_68_369_2300_097, and the Program Management Unit for Human Resources & Institutional Development, Research and Innovation, grant B39G680009 (Thailand); the Kavli Foundation; the Nvidia Corporation; the SuperMicro Corporation; the Welch Foundation, contract C-1845; and the Weston Havens Foundation (U.S.A.).

Data Availability Statement. Release and preservation of data used by the CMS Collaboration as the basis for publications is guided by the CMS data preservation, re-use and open access policy.

Code Availability Statement. The CMS core software is publicly available on GitHub.

References

[1] K. Hagiwara, R.D. Peccei, D. Zeppenfeld and K. Hikasa, *Probing the Weak Boson Sector in* $e^+e^- \to W^+W^-$, *Nucl. Phys. B* **282** (1987) 253 [INSPIRE].

[2] U. Baur and E.L. Berger, *Probing the weak boson sector in* $Z\gamma$ *production at hadron colliders*, *Phys. Rev. D* **47** (1993) 4889 [INSPIRE].

[3] U. Baur, T. Han and J. Ohnemus, *QCD corrections and anomalous couplings in* $Z\gamma$ *production at hadron colliders*, *Phys. Rev. D* **57** (1998) 2823 [hep-ph/9710416] [INSPIRE].

[4] G.J. Gounaris, J. Layssac and F.M. Renard, *Signatures of the anomalous Z_γ and ZZ production at the lepton and hadron colliders*, Phys. Rev. D **61** (2000) 073013 [hep-ph/9910395] [INSPIRE].

[5] B. Bellazzini and F. Riva, *New phenomenological and theoretical perspective on anomalous ZZ and $Z\gamma$ processes*, Phys. Rev. D **98** (2018) 095021 [arXiv:1806.09640] [INSPIRE].

[6] J. Ellis, H.-J. He and R.-Q. Xiao, *Probing neutral triple gauge couplings at the LHC and future hadron colliders*, Phys. Rev. D **107** (2023) 035005 [arXiv:2206.11676] [INSPIRE].

[7] CMS collaboration, *Measurement of $Z\gamma$ production in proton-proton collisions at $\sqrt{s} = 13.6$ TeV and constraints on neutral triple gauge couplings*, arXiv:2512.08582 [INSPIRE].

[8] D0 collaboration, *Study of $Z\gamma$ events and limits on anomalous $ZZ\gamma$ and $Z\gamma\gamma$ couplings in $p\bar{p}$ collisions at $\sqrt{s} = 1.96$-TeV*, Phys. Rev. Lett. **95** (2005) 051802 [hep-ex/0502036] [INSPIRE].

[9] CDF collaboration, *Measurement of $Z\gamma$ Production in $p\bar{p}$ Collisions at $\sqrt{s} = 1.96$ TeV*, Phys. Rev. D **82** (2010) 031103 [arXiv:1004.1140] [INSPIRE].

[10] CDF collaboration, *Limits on Anomalous Trilinear Gauge Couplings in $Z\gamma$ Events from $p\bar{p}$ Collisions at $\sqrt{s} = 1.96$ TeV*, Phys. Rev. Lett. **107** (2011) 051802 [arXiv:1103.2990] [INSPIRE].

[11] CMS collaboration, *Measurement of the $Z\gamma$ production cross section in pp collisions at $\sqrt{s} = 8$ TeV and search for anomalous triple gauge boson couplings*, JHEP **04** (2015) 164 [arXiv:1502.05664] [INSPIRE].

[12] CMS collaboration, *Measurement of the $Z\gamma \to \nu\bar{\nu}\gamma$ production cross section in pp collisions at $\sqrt{s} = 8$ TeV and limits on anomalous $ZZ\gamma$ and $Z\gamma\gamma$ trilinear gauge boson couplings*, Phys. Lett. B **760** (2016) 448 [arXiv:1602.07152] [INSPIRE].

[13] ATLAS collaboration, *Measurements of $Z\gamma$ and $Z\gamma\gamma$ production in pp collisions at $\sqrt{s} = 8$ TeV with the ATLAS detector*, Phys. Rev. D **93** (2016) 112002 [arXiv:1604.05232] [INSPIRE].

[14] ATLAS collaboration, *Measurement of the $Z\gamma \to \nu\bar{\nu}\gamma$ production cross section in pp collisions at $\sqrt{s} = 13$ TeV with the ATLAS detector and limits on anomalous triple gauge-boson couplings*, JHEP **12** (2018) 010 [arXiv:1810.04995] [INSPIRE].

[15] D0 collaboration, *$Z\gamma$ production and limits on anomalous $ZZ\gamma$ and $Z\gamma\gamma$ couplings in $p\bar{p}$ collisions at $\sqrt{s} = 1.96$ TeV*, Phys. Lett. B **653** (2007) 378 [arXiv:0705.1550] [INSPIRE].

[16] ATLAS collaboration, *Measurement of $W\gamma$ and $Z\gamma$ production in proton-proton collisions at $\sqrt{s} = 7$ TeV with the ATLAS detector*, JHEP **09** (2011) 072 [arXiv:1106.1592] [INSPIRE].

[17] HEPData record for this analysis, DOI:10.17182/hepdata.167736 (2026).

[18] CMS collaboration, *The CMS Experiment at the CERN LHC*, 2008 JINST **3** S08004 [INSPIRE].

[19] CMS collaboration, *Development of the CMS detector for the CERN LHC Run 3*, 2024 JINST **19** P05064 [arXiv:2309.05466] [INSPIRE].

[20] CMS collaboration, *Performance of the CMS Level-1 trigger in proton-proton collisions at $\sqrt{s} = 13$ TeV*, 2020 JINST **15** P10017 [arXiv:2006.10165] [INSPIRE].

[21] CMS collaboration, *The CMS trigger system*, 2017 JINST **12** P01020 [arXiv:1609.02366] [INSPIRE].

[22] CMS collaboration, *Performance of the CMS high-level trigger during LHC Run 2*, 2024 JINST **19** P11021 [arXiv:2410.17038] [INSPIRE].

[23] CMS collaboration, *Electron and photon reconstruction and identification with the CMS experiment at the CERN LHC*, 2021 JINST **16** P05014 [arXiv:2012.06888] [INSPIRE].

[24] CMS collaboration, *Performance of the CMS muon detector and muon reconstruction with proton-proton collisions at $\sqrt{s} = 13$ TeV*, 2018 *JINST* **13** P06015 [arXiv:1804.04528] [INSPIRE].

[25] CMS collaboration, *Description and Performance of Track and Primary-Vertex Reconstruction with the CMS Tracker*, 2014 *JINST* **9** P10009 [arXiv:1405.6569] [INSPIRE].

[26] CMS collaboration, *Particle-flow reconstruction and global event description with the CMS detector*, 2017 *JINST* **12** P10003 [arXiv:1706.04965] [INSPIRE].

[27] CMS collaboration, *Technical proposal for the Phase-II upgrade of the Compact Muon Solenoid*, CMS-TDR-15-02 (2015).

[28] M. Cacciari, G.P. Salam and G. Soyez, *The anti-k_t jet clustering algorithm*, *JHEP* **04** (2008) 063 [arXiv:0802.1189] [INSPIRE].

[29] M. Cacciari, G.P. Salam and G. Soyez, *FastJet User Manual*, *Eur. Phys. J. C* **72** (2012) 1896 [arXiv:1111.6097] [INSPIRE].

[30] CMS collaboration, *Pileup mitigation at CMS in 13 TeV data*, 2020 *JINST* **15** P09018 [arXiv:2003.00503] [INSPIRE].

[31] CMS collaboration, *Jet energy scale and resolution in the CMS experiment in pp collisions at 8 TeV*, 2017 *JINST* **12** P02014 [arXiv:1607.03663] [INSPIRE].

[32] CMS collaboration, *Performance of missing transverse momentum reconstruction in proton-proton collisions at $\sqrt{s} = 13$ TeV using the CMS detector*, 2019 *JINST* **14** P07004 [arXiv:1903.06078] [INSPIRE].

[33] CMS collaboration, *Measurements of Inclusive W and Z Cross Sections in pp Collisions at $\sqrt{s} = 7$ TeV*, *JHEP* **01** (2011) 080 [arXiv:1012.2466] [INSPIRE].

[34] A. Bodek et al., *Extracting Muon Momentum Scale Corrections for Hadron Collider Experiments*, *Eur. Phys. J. C* **72** (2012) 2194 [arXiv:1208.3710] [INSPIRE].

[35] CMS collaboration, *Mitigation of anomalous APD signals in the CMS electromagnetic calorimeter*, *J. Phys. Conf. Ser.* **404** (2012) 012043 [INSPIRE].

[36] A.P. Singh, P.C. Bhat, N.V. Mokhov and S. Beri, *Beam-induced radiation in the compact muon solenoid tracker at the Large Hadron Collider*, *Pramana* **74** (2010) 719 [INSPIRE].

[37] J. Alwall et al., *The automated computation of tree-level and next-to-leading order differential cross sections, and their matching to parton shower simulations*, *JHEP* **07** (2014) 079 [arXiv:1405.0301] [INSPIRE].

[38] CMS collaboration, *Extraction and validation of a new set of CMS PYTHIA8 tunes from underlying-event measurements*, *Eur. Phys. J. C* **80** (2020) 4 [arXiv:1903.12179] [INSPIRE].

[39] T. Sjöstrand et al., *An introduction to PYTHIA 8.2*, *Comput. Phys. Commun.* **191** (2015) 159 [arXiv:1410.3012] [INSPIRE].

[40] GEANT4 collaboration, *GEANT4 — A Simulation Toolkit*, *Nucl. Instrum. Meth. A* **506** (2003) 250 [INSPIRE].

[41] M. Grazzini, S. Kallweit and D. Rathlev, *$W\gamma$ and $Z\gamma$ production at the LHC in NNLO QCD*, *JHEP* **07** (2015) 085 [arXiv:1504.01330] [INSPIRE].

[42] A. Denner, S. Dittmaier, M. Hecht and C. Pasold, *NLO QCD and electroweak corrections to $Z + \gamma$ production with leptonic Z-boson decays*, *JHEP* **02** (2016) 057 [arXiv:1510.08742] [INSPIRE].

[43] A. Denner, S. Dittmaier, M. Hecht and C. Pasold, *NLO QCD and electroweak corrections to* $W+\gamma$ *production with leptonic W-boson decays*, *JHEP* **04** (2015) 018 [arXiv:1412.7421] [INSPIRE].

[44] NNPDF collaboration, *Illuminating the photon content of the proton within a global PDF analysis*, *SciPost Phys.* **5** (2018) 008 [arXiv:1712.07053] [INSPIRE].

[45] M.A. Wadud, *Measurements on the production of a Z boson in association with a photon in proton-proton collisions and a search for anomalous triple gauge couplings at the CERN Large Hadron Collider*, Ph.D. thesis, 2023-07-31, Minnesota University, U.S.A. (2023) [INSPIRE].

[46] CMS collaboration, *Muon reconstruction and identification performance with Run-2 data*, CMS-DP-2020-040 (2020).

[47] CMS collaboration, *Search for new physics in final states with a single photon and missing transverse momentum in proton-proton collisions at* $\sqrt{s}=13$ *TeV*, *JHEP* **02** (2019) 074 [arXiv:1810.00196] [INSPIRE].

[48] CMS collaboration, *Precision luminosity measurement in proton-proton collisions at* $\sqrt{s}=13$ *TeV in 2015 and 2016 at CMS*, *Eur. Phys. J. C* **81** (2021) 800 [arXiv:2104.01927] [INSPIRE].

[49] CMS collaboration, *CMS luminosity measurement for the 2017 data-taking period at* $\sqrt{s}=13$ *TeV*, CMS-PAS-LUM-17-004 (2018).

[50] CMS collaboration, *CMS luminosity measurement for the 2018 data-taking period at* $\sqrt{s}=13$ *TeV*, CMS-PAS-LUM-18-002 (2019).

[51] CMS collaboration, *Measurement of the inelastic proton-proton cross section at* $\sqrt{s}=13$ *TeV*, *JHEP* **07** (2018) 161 [arXiv:1802.02613] [INSPIRE].

[52] M. Grazzini, S. Kallweit and M. Wiesemann, *Fully differential NNLO computations with MATRIX*, *Eur. Phys. J. C* **78** (2018) 537 [arXiv:1711.06631] [INSPIRE].

[53] J.M. Lindert et al., *Precise predictions for* $V+$ *jets dark matter backgrounds*, *Eur. Phys. J. C* **77** (2017) 829 [arXiv:1705.04664] [INSPIRE].

[54] J. Butterworth et al., *PDF4LHC recommendations for LHC Run II*, *J. Phys. G* **43** (2016) 023001 [arXiv:1510.03865] [INSPIRE].

[55] CMS collaboration, *The CMS Statistical Analysis and Combination Tool: Combine*, *Comput. Softw. Big Sci.* **8** (2024) 19 [arXiv:2404.06614] [INSPIRE].

[56] R.J. Barlow and C. Beeston, *Fitting using finite Monte Carlo samples*, *Comput. Phys. Commun.* **77** (1993) 219 [INSPIRE].

[57] A. Gaponenko, *A Practical Way to Regularize Unfolding of Sharply Varying Spectra with Low Data Statistics*, *Nucl. Instrum. Meth. A* **960** (2020) 163612 [arXiv:1906.07918] [INSPIRE].

[58] B. Pollack, S. Bhattacharya and M. Schmitt, *Bayesian Block Histogramming for High Energy Physics*, arXiv:1708.00810 [INSPIRE].

JHEP08(2026)049

The CMS collaboration

A. Hayrapetyan[1], A. Tumasyan[1,a], W. Adam[2], J.W. Andrejkovic[2], T. Bergauer[2], S. Chatterjee[2], K. Damanakis[2], M. Dragicevic[2], P.S. Hussain[2], M. Jeitler[2,b], N. Krammer[2], A. Li[2], D. Liko[2], I. Mikulec[2], J. Schieck[2,b], R. Schöfbeck[2,b], D. Schwarz[2], M. Sonawane[2], W. Waltenberger[2], C.-E. Wulz[2,b], T. Janssen[3], T. Van Laer[3], P. Van Mechelen[3], N. Breugelmans[4], J. D'Hondt[4], S. Dansana[4], A. De Moor[4], M. Delcourt[4], F. Heyen[4], S. Lowette[4], I. Makarenko[4], D. Müller[4], S. Tavernier[4], M. Tytgat[4,c], G.P. Van Onsem[4], S. Van Putte[4], D. Vannerom[4], B. Bilin[5], B. Clerbaux[5], A.K. Das[5], G. De Lentdecker[5], H. Evard[5], L. Favart[5], P. Gianneios[5], J. Jaramillo[5], A. Khalilzadeh[5], F.A. Khan[5], K. Lee[5], M. Mahdavikhorrami[5], A. Malara[5], S. Paredes[5], M.A. Shahzad[5], L. Thomas[5], M. Vanden Bemden[5], C. Vander Velde[5], P. Vanlaer[5], M. De Coen[6], D. Dobur[6], G. Gokbulut[6], Y. Hong[6], J. Knolle[6], L. Lambrecht[6], D. Marckx[6], K. Mota Amarilo[6], K. Skovpen[6], N. Van Den Bossche[6], J. van der Linden[6], L. Wezenbeek[6], A. Benecke[7], A. Bethani[7], G. Bruno[7], C. Caputo[7], J. De Favereau De Jeneret[7], C. Delaere[7], I.S. Donertas[7], A. Giammanco[7], A.O. Guzel[7], Sa. Jain[7], V. Lemaitre[7], J. Lidrych[7], P. Mastrapasqua[7], T.T. Tran[7], G.A. Alves[8], M. Alves Gallo Pereira[8], E. Coelho[8], G. Correia Silva[8], C. Hensel[8], T. Menezes De Oliveira[8], C. Mora Herrera[8,d], P. Rebello Teles[8], M. Soeiro[8], A. Vilela Pereira[8,d], W.L. Aldá Júnior[9], M. Barroso Ferreira Filho[9], H. Brandao Malbouisson[9], W. Carvalho[9], J. Chinellato[9,e], E.M. Da Costa[9], G.G. Da Silveira[9,f], D. De Jesus Damiao[9], S. Fonseca De Souza[9], R. Gomes De Souza[9], T. Laux Kuhn[9], M. Macedo[9], J. Martins[9,g], L. Mundim[9], H. Nogima[9], J.P. Pinheiro[9], A. Santoro[9], A. Sznajder[9], M. Thiel[9], C.A. Bernardes[10,f], L. Calligaris[10], T.R. Fernandez Perez Tomei[10], E.M. Gregores[10], I. Maietto Silverio[10], P.G. Mercadante[10], S.F. Novaes[10], B. Orzari[10], Sandra S. Padula[10], A. Aleksandrov[11], G. Antchev[11], R. Hadjiiska[11], P. Iaydjiev[11], M. Misheva[11], M. Shopova[11], G. Sultanov[11], A. Dimitrov[12], L. Litov[12], B. Pavlov[12], P. Petkov[12], A. Petrov[12], E. Shumka[12], S. Keshri[13], D. Laroze[13], S. Thakur[13], T. Cheng[14], T. Javaid[14], L. Yuan[14], Z. Hu[15], Z. Liang[15], J. Liu[15], G.M. Chen[16,h], H.S. Chen[16,h], M. Chen[16,h], F. Iemmi[16], C.H. Jiang[16], A. Kapoor[16,i], H. Liao[16], Z.-A. Liu[16,j], R. Sharma[16,k], J.N. Song[16,j], J. Tao[16], C. Wang[16,h], J. Wang[16], Z. Wang[16,h], H. Zhang[16], J. Zhao[16], A. Agapitos[17], Y. Ban[17], A. Carvalho Antunes De Oliveira[17], S. Deng[17], B. Guo[17], C. Jiang[17], A. Levin[17], C. Li[17], Q. Li[17], Y. Mao[17], S. Qian[17], S.J. Qian[17], X. Qin[17], X. Sun[17], D. Wang[17], H. Yang[17], L. Zhang[17], Y. Zhao[17], C. Zhou[17], S. Yang[18], Z. You[19], K. Jaffel[20], N. Lu[20], G. Bauer[21,l], B. Li[21,m], K. Yi[21,n], J. Zhang[21], Y. Li[22], Z. Lin[23], C. Lu[23], M. Xiao[23], C. Avila[24], D.A. Barbosa Trujillo[24], A. Cabrera[24], C. Florez[24], J. Fraga[24], J.A. Reyes Vega[24], F. Ramirez[25], C. Rendón[25], M. Rodriguez[25], A.A. Ruales Barbosa[25], J.D. Ruiz Alvarez[25], D. Giljanovic[26], N. Godinovic[26], D. Lelas[26], A. Sculac[26], M. Kovac[27], A. Petkovic[27], T. Sculac[27], P. Bargassa[28], V. Brigljevic[28], B.K. Chitroda[28], D. Ferencek[28], K. Jakovcic[28], A. Starodumov[28,o], T. Susa[28], A. Attikis[29], K. Christoforou[29], A. Hadjiagapiou[29], C. Leonidou[29], J. Mousa[29], C. Nicolaou[29], L. Paizanos[29], F. Ptochos[29], P.A. Razis[29], H. Rykaczewski[29], H. Saka[29], A. Stepennov[29], M. Finger[30], M. Finger Jr.[30], A. Kveton[30], E. Carrera Jarrin[31], H. Abdalla[32,p],

JHEP08(2026)049

S. Abu Zeid[32,q], Y. Assran[32,r,s], M.A. Mahmoud[33], Y. Mohammed[33], K. Ehataht[34], M. Kadastik[34], T. Lange[34], S. Nandan[34], C. Nielsen[34], J. Pata[34], M. Raidal[34], L. Tani[34], C. Veelken[34], H. Kirschenmann[35], K. Osterberg[35], M. Voutilainen[35], S. Bharthuar[36], N. Bin Norjoharuddeen[36], E. Brücken[36], F. Garcia[36], P. Inkaew[36], K.T.S. Kallonen[36], T. Lampén[36], K. Lassila-Perini[36], S. Lehti[36], T. Lindén[36], M. Myllymäki[36], M.m. Rantanen[36], H. Siikonen[36], J. Tuominiemi[36], P. Luukka[37], H. Petrow[37], M. Besancon[38], F. Couderc[38], M. Dejardin[38], D. Denegri[38], J.L. Faure[38], F. Ferri[38], S. Ganjour[38], P. Gras[38], G. Hamel de Monchenault[38], M. Kumar[38], V. Lohezic[38], J. Malcles[38], F. Orlandi[38], L. Portales[38], A. Rosowsky[38], M.Ö. Sahin[38], A. Savoy-Navarro[38,t], P. Simkina[38], M. Titov[38], M. Tornago[38], F. Beaudette[39], G. Boldrini[39], P. Busson[39], A. Cappati[39], C. Charlot[39], M. Chiusi[39], T.D. Cuisset[39], F. Damas[39], O. Davignon[39], A. De Wit[39], I.T. Ehle[39], B.A. Fontana Santos Alves[39], S. Ghosh[39], A. Gilbert[39], R. Granier de Cassagnac[39], A. Hakimi[39], B. Harikrishnan[39], L. Kalipoliti[39], G. Liu[39], M. Nguyen[39], C. Ochando[39], R. Salerno[39], J.B. Sauvan[39], Y. Sirois[39], L. Urda Gómez[39], E. Vernazza[39], A. Zabi[39], A. Zghiche[39], J.-L. Agram[40,u], J. Andrea[40], D. Apparu[40], D. Bloch[40], J.-M. Brom[40], E.C. Chabert[40], C. Collard[40], S. Falke[40], U. Goerlach[40], R. Haeberle[40], A.-C. Le Bihan[40], M. Meena[40], O. Poncet[40], G. Saha[40], M.A. Sessini[40], P. Van Hove[40], P. Vaucelle[40], A. Di Florio[41], D. Amram[42], S. Beauceron[42], B. Blancon[42], G. Boudoul[42], N. Chanon[42], D. Contardo[42], P. Depasse[42], C. Dozen[42,v], H. El Mamouni[42], J. Fay[42], S. Gascon[42], M. Gouzevitch[42], C. Greenberg[42], G. Grenier[42], B. Ille[42], E. Jourd'huy[42], I.B. Laktineh[42], M. Lethuillier[42], L. Mirabito[42], S. Perries[42], A. Purohit[42], M. Vander Donckt[42], P. Verdier[42], J. Xiao[42], G. Adamov[43], I. Lomidze[43], Z. Tsamalaidze[43,w], V. Botta[44], S. Consuegra Rodríguez[44], L. Feld[44], K. Klein[44], M. Lipinski[44], D. Meuser[44], A. Pauls[44], D. Pérez Adán[44], N. Röwert[44], M. Teroerde[44], S. Diekmann[45], A. Dodonova[45], N. Eich[45], D. Eliseev[45], F. Engelke[45], J. Erdmann[45], M. Erdmann[45], P. Fackeldey[45], B. Fischer[45], T. Hebbeker[45], K. Hoepfner[45], F. Ivone[45], A. Jung[45], M.y. Lee[45], F. Mausolf[45], M. Merschmeyer[45], A. Meyer[45], S. Mukherjee[45], D. Noll[45], F. Nowotny[45], A. Pozdnyakov[45], Y. Rath[45], W. Redjeb[45], F. Rehm[45], H. Reithler[45], V. Sarkisovi[45], A. Schmidt[45], C. Seth[45], A. Sharma[45], J.L. Spah[45], A. Stein[45], F. Torres Da Silva De Araujo[45,x], S. Wiedenbeck[45], S. Zaleski[45], C. Dziwok[46], G. Flügge[46], T. Kress[46], A. Nowack[46], O. Pooth[46], A. Stahl[46], T. Ziemons[46], A. Zotz[46], H. Aarup Petersen[47], M. Aldaya Martin[47], J. Alimena[47], S. Amoroso[47], Y. An[47], J. Bach[47], S. Baxter[47], M. Bayatmakou[47], H. Becerril Gonzalez[47], O. Behnke[47], A. Belvedere[47], F. Blekman[47,y], K. Borras[47,z], A. Campbell[47], A. Cardini[47], C. Cheng[47], F. Colombina[47], G. Eckerlin[47], D. Eckstein[47], L.I. Estevez Banos[47], O. Filatov[47], E. Gallo[47,y], A. Geiser[47], V. Guglielmi[47], M. Guthoff[47], A. Hinzmann[47], L. Jeppe[47], B. Kaech[47], M. Kasemann[47], C. Kleinwort[47], R. Kogler[47], M. Komm[47], D. Krücker[47], W. Lange[47], D. Leyva Pernia[47], K. Lipka[47,aa], W. Lohmann[47,ab], F. Lorkowski[47], R. Mankel[47], I.-A. Melzer-Pellmann[47], M. Mendizabal Morentin[47], A.B. Meyer[47], G. Milella[47], K. Moral Figueroa[47], A. Mussgiller[47], L.P. Nair[47], J. Niedziela[47], A. Nürnberg[47], Y. Otarid[47], J. Park[47], E. Ranken[47], A. Raspereza[47], D. Rastorguev[47], J. Rübenach[47], L. Rygaard[47], A. Saggio[47], M. Scham[47,ac,ad], S. Schnake[47,z], P. Schütze[47], C. Schwanenberger[47,y], D. Selivanova[47],

JHEP08(2026)049

K. Sharko[47], M. Shchedrolosiev[47], D. Stafford[47], F. Vazzoler[47], A. Ventura Barroso[47], R. Walsh[47], D. Wang[47], Q. Wang[47], Y. Wen[47], K. Wichmann[47], L. Wiens[47,z], C. Wissing[47], Y. Yang[47], A. Zimermmane Castro Santos[47], A. Albrecht[48], S. Albrecht[48], M. Antonello[48], S. Bein[48], L. Benato[48], S. Bollweg[48], M. Bonanomi[48], P. Connor[48], K. El Morabit[48], Y. Fischer[48], E. Garutti[48], A. Grohsjean[48], J. Haller[48], D. Hundhausen[48], H.R. Jabusch[48], G. Kasieczka[48], P. Keicher[48], R. Klanner[48], W. Korcari[48], T. Kramer[48], C.c. Kuo[48], V. Kutzner[48], F. Labe[48], J. Lange[48], A. Lobanov[48], C. Matthies[48], L. Moureaux[48], M. Mrowietz[48], A. Nigamova[48], Y. Nissan[48], A. Paasch[48], K.J. Pena Rodriguez[48], T. Quadfasel[48], B. Raciti[48], M. Rieger[48], D. Savoiu[48], J. Schindler[48], P. Schleper[48], M. Schröder[48], J. Schwandt[48], M. Sommerhalder[48], H. Stadie[48], G. Steinbrück[48], A. Tews[48], B. Wiederspan[48], M. Wolf[48], S. Brommer[49], E. Butz[49], T. Chwalek[49], A. Dierlamm[49], A. Droll[49], U. Elicabuk[49], N. Faltermann[49], M. Giffels[49], A. Gottmann[49], F. Hartmann[49,ae], R. Hofsaess[49], M. Horzela[49], U. Husemann[49], J. Kieseler[49], M. Klute[49], R. Koppenhöfer[49], O. Lavoryk[49], J.M. Lawhorn[49], M. Link[49], A. Lintuluoto[49], S. Maier[49], S. Mitra[49], M. Mormile[49], Th. Müller[49], M. Neukum[49], M. Oh[49], E. Pfeffer[49], M. Presilla[49], G. Quast[49], K. Rabbertz[49], B. Regnery[49], N. Shadskiy[49], I. Shvetsov[49], H.J. Simonis[49], L. Sowa[49], L. Stockmeier[49], K. Tauqeer[49], M. Toms[49], N. Trevisani[49], R.F. Von Cube[49], M. Wassmer[49], S. Wieland[49], F. Wittig[49], R. Wolf[49], X. Zuo[49], G. Anagnostou[50], G. Daskalakis[50], A. Kyriakis[50], A. Papadopoulos[50,ae], A. Stakia[50], P. Kontaxakis[51], G. Melachroinos[51], Z. Painesis[51], I. Papavergou[51], I. Paraskevas[51], N. Saoulidou[51], K. Theofilatos[51], E. Tziaferi[51], K. Vellidis[51], I. Zisopoulos[51], G. Bakas[52], T. Chatzistavrou[52], G. Karapostoli[52], K. Kousouris[52], I. Papakrivopoulos[52], E. Siamarkou[52], G. Tsipolitis[52], A. Zacharopoulou[52], I. Bestintzanos[53], I. Evangelou[53], C. Foudas[53], C. Kamtsikis[53], P. Katsoulis[53], P. Kokkas[53], P.G. Kosmoglou Kioseoglou[53], N. Manthos[53], I. Papadopoulos[53], J. Strologas[53], C. Hajdu[54], D. Horvath[54,af,ag], K. Márton[54], A.J. Rádl[54,ah], F. Sikler[54], V. Veszpremi[54], M. Csanád[55], K. Farkas[55], A. Fehérkuti[55,ai], M.M.A. Gadallah[55,aj], Á. Kadlecsik[55], P. Major[55], G. Pásztor[55], G.I. Veres[55], B. Ujvari[56], G. Zilizi[56], G. Bencze[57], S. Czellar[57], J. Molnar[57], Z. Szillasi[57], T. Csorgo[58,ai], F. Nemes[58,ai], T. Novak[58], S. Bansal[59], S.B. Beri[59], V. Bhatnagar[59], G. Chaudhary[59], S. Chauhan[59], N. Dhingra[59,ak], A. Kaur[59], A. Kaur[59], H. Kaur[59], M. Kaur[59], S. Kumar[59], T. Sheokand[59], J.B. Singh[59], A. Singla[59], A. Ahmed[60], A. Bhardwaj[60], A. Chhetri[60], B.C. Choudhary[60], A. Kumar[60], A. Kumar[60], M. Naimuddin[60], K. Ranjan[60], M.K. Saini[60], S. Saumya[60], S. Baradia[61], S. Barman[61,al], S. Bhattacharya[61], S. Das Gupta[61], S. Dutta[61], S. Dutta[61], S. Sarkar[61], M.M. Ameen[62], P.K. Behera[62], S.C. Behera[62], S. Chatterjee[62], G. Dash[62], P. Jana[62], P. Kalbhor[62], S. Kamble[62], J.R. Komaragiri[62,am], D. Kumar[62,am], T. Mishra[62], B. Parida[62], P.R. Pujahari[62], N.R. Saha[62], A. Sharma[62], A.K. Sikdar[62], R.K. Singh[62], P. Verma[62], S. Verma[62], A. Vijay[62], S. Dugad[63], G.B. Mohanty[63], M. Shelake[63], P. Suryadevara[63], A. Bala[64], S. Banerjee[64], R.M. Chatterjee[64], M. Guchait[64], Sh. Jain[64], A. Jaiswal[64], S. Kumar[64], G. Majumder[64], K. Mazumdar[64], S. Parolia[64], A. Thachayath[64], S. Bahinipati[65,an], C. Kar[65], D. Maity[65,ao], P. Mal[65], V.K. Muraleedharan Nair Bindhu[65,ao], K. Naskar[65,ao], A. Nayak[65,ao], S. Nayak[65], K. Pal[65], P. Sadangi[65], S.K. Swain[65], S. Varghese[65,ao],

D. Vats[65,ao], S. Acharya[66,ap], A. Alpana[66], S. Dube[66], B. Gomber[66,ap], P. Hazarika[66], B. Kansal[66], A. Laha[66], B. Sahu[66,ap], S. Sharma[66], K.Y. Vaish[66], H. Bakhshiansohi[67,aq], A. Jafari[67,ar], M. Zeinali[67,as], S. Bashiri[68], S. Chenarani[68,at], S.M. Etesami[68], Y. Hosseini[68], M. Khakzad[68], E. Khazaie[68], M. Mohammadi Najafabadi[68], S. Tizchang[68,au], M. Felcini[69], M. Grunewald[69], M. Abbrescia[70a,70b], A. Colaleo[70a,70b], D. Creanza[70a,70c], B. D'Anzi[70a,70b], N. De Filippis[70a,70c], M. De Palma[70a,70b], W. Elmetenawee[70a,70b,av], N. Ferrara[70a,70b], L. Fiore[70a], G. Iaselli[70a,70c], L. Longo[70a], M. Louka[70a,70b], G. Maggi[70a,70c], M. Maggi[70a], I. Margjeka[70a], V. Mastrapasqua[70a,70b], S. My[70a,70b], S. Nuzzo[70a,70b], A. Pellecchia[70a,70b], A. Pompili[70a,70b], G. Pugliese[70a,70c], R. Radogna[70a,70b], D. Ramos[70a], A. Ranieri[70a], L. Silvestris[70a], F.M. Simone[70a,70c], Ü. Sözbilir[70a], A. Stamerra[70a,70b], D. Troiano[70a,70b], R. Venditti[70a,70b], P. Verwilligen[70a], A. Zaza[70a,70b], G. Abbiendi[71a], C. Battilana[71a,71b], D. Bonacorsi[71a,71b], P. Capiluppi[71a,71b], A. Castro[71a,71b,†], F.R. Cavallo[71a], M. Cuffiani[71a,71b], G.M. Dallavalle[71a], T. Diotalevi[71a,71b], F. Fabbri[71a], A. Fanfani[71a,71b], D. Fasanella[71a], P. Giacomelli[71a], L. Giommi[71a,71b], C. Grandi[71a], L. Guiducci[71a,71b], S. Lo Meo[71a,aw], M. Lorusso[71a,71b], L. Lunerti[71a], S. Marcellini[71a], G. Masetti[71a], F.L. Navarria[71a,71b], G. Paggi[71a,71b], A. Perrotta[71a], F. Primavera[71a,71b], A.M. Rossi[71a,71b], S. Rossi Tisbeni[71a,71b], T. Rovelli[71a,71b], G.P. Siroli[71a,71b], S. Costa[72a,72b,ax], A. Di Mattia[72a], A. Lapertosa[72a], R. Potenza[72a,72b], A. Tricomi[72a,72b,ax], C. Tuve[72a,72b], P. Assiouras[73a], G. Barbagli[73a], G. Bardelli[73a,73b], B. Camaiani[73a,73b], A. Cassese[73a], R. Ceccarelli[73a], V. Ciulli[73a,73b], C. Civinini[73a], R. D'Alessandro[73a,73b], E. Focardi[73a,73b], T. Kello[73a], G. Latino[73a,73b], P. Lenzi[73a,73b], M. Lizzo[73a], M. Meschini[73a], S. Paoletti[73a], A. Papanastassiou[73a,73b], G. Sguazzoni[73a], L. Viliani[73a], L. Benussi[74], S. Bianco[74], S. Meola[74,ay], D. Piccolo[74], F. Ferro[75a], E. Robutti[75a], S. Tosi[75a,75b], A. Benaglia[76a], F. Brivio[76a], F. Cetorelli[76a,76b], F. De Guio[76a,76b], M.E. Dinardo[76a,76b], P. Dini[76a], S. Gennai[76a], R. Gerosa[76a,76b], A. Ghezzi[76a,76b], P. Govoni[76a,76b], L. Guzzi[76a], M.T. Lucchini[76a,76b], M. Malberti[76a], S. Malvezzi[76a], A. Massironi[76a], D. Menasce[76a], L. Moroni[76a], M. Paganoni[76a,76b], S. Palluotto[76a,76b], D. Pedrini[76a], A. Perego[76a,76b], B.S. Pinolini[76a], G. Pizzati[76a,76b], S. Ragazzi[76a,76b], T. Tabarelli de Fatis[76a,76b], S. Buontempo[77a], A. Cagnotta[77a,77b], F. Carnevali[77a,77b], N. Cavallo[77a,77c], F. Fabozzi[77a,77c], A.O.M. Iorio[77a,77b], L. Lista[77a,77b,az], P. Paolucci[77a,ae], B. Rossi[77a], R. Ardino[78a], P. Azzi[78a], N. Bacchetta[78a,ba], D. Bisello[78a,78b], P. Bortignon[78a], G. Bortolato[78a,78b], A. Bragagnolo[78a,78b], A.C.M. Bulla[78a], R. Carlin[78a,78b], P. Checchia[78a], T. Dorigo[78a,bb], F. Gasparini[78a,78b], U. Gasparini[78a,78b], S. Giorgetti[78a], E. Lusiani[78a], M. Margoni[78a,78b], M. Migliorini[78a,78b], J. Pazzini[78a,78b], P. Ronchese[78a,78b], R. Rossin[78a,78b], M. Sgaravatto[78a], F. Simonetto[78a,78b], M. Tosi[78a,78b], A. Triossi[78a,78b], S. Ventura[78a], M. Zanetti[78a,78b], P. Zotto[78a,78b], A. Zucchetta[78a,78b], G. Zumerle[78a,78b], A. Braghieri[79a], S. Calzaferri[79a], D. Fiorina[79a], P. Montagna[79a,79b], V. Re[79a], C. Riccardi[79a,79b], P. Salvini[79a], I. Vai[79a,79b], P. Vitulo[79a,79b], S. Ajmal[80a,80b], M.E. Ascioti[80a,80b], G.M. Bilei[80a], C. Carrivale[80a,80b], D. Ciangottini[80a,80b], L. Fanò[80a,80b], M. Magherini[80a,80b], V. Mariani[80a,80b], M. Menichelli[80a], F. Moscatelli[80a,bc], A. Rossi[80a,80b], A. Santocchia[80a,80b], D. Spiga[80a], T. Tedeschi[80a,80b], C. Aimè[81a], C.A. Alexe[81a,81c], P. Asenov[81a,81b], P. Azzurri[81a], G. Bagliesi[81a], R. Bhattacharya[81a],

JHEP08(2026)049

L. Bianchini[81a,81b], T. Boccali[81a], E. Bossini[81a], D. Bruschini[81a,81c], R. Castaldi[81a], M.A. Ciocci[81a,81b], M. Cipriani[81a,81b], V. D'Amante[81a,81d], R. Dell'Orso[81a], S. Donato[81a], A. Giassi[81a], F. Ligabue[81a,81c], A.C. Marini[81a,81b], D. Matos Figueiredo[81a], A. Messineo[81a,81b], S. Mishra[81a], M. Musich[81a,81b], F. Palla[81a], A. Rizzi[81a,81b], G. Rolandi[81a,81c], S. Roy Chowdhury[81a], T. Sarkar[81a], A. Scribano[81a], P. Spagnolo[81a], R. Tenchini[81a], G. Tonelli[81a,81b], N. Turini[81a,81d], F. Vaselli[81a,81c], A. Venturi[81a], P.G. Verdini[81a], C. Baldenegro Barrera[82a,82b], P. Barria[82a], C. Basile[82a,82b], F. Cavallari[82a], L. Cunqueiro Mendez[82a,82b], D. Del Re[82a,82b], E. Di Marco[82a,82b], M. Diemoz[82a], F. Errico[82a,82b], R. Gargiulo[82a,82b], E. Longo[82a,82b], L. Martikainen[82a,82b], J. Mijuskovic[82a,82b], G. Organtini[82a,82b], F. Pandolfi[82a], R. Paramatti[82a,82b], C. Quaranta[82a,82b], S. Rahatlou[82a,82b], C. Rovelli[82a], F. Santanastasio[82a,82b], L. Soffi[82a], V. Vladimirov[82a,82b], N. Amapane[83a,83b], R. Arcidiacono[83a,83c], S. Argiro[83a,83b], M. Arneodo[83a,83c], N. Bartosik[83a], R. Bellan[83a,83b], A. Bellora[83a,83b], C. Biino[83a], C. Borca[83a,83b], N. Cartiglia[83a], M. Costa[83a,83b], R. Covarelli[83a,83b], N. Demaria[83a], L. Finco[83a], M. Grippo[83a,83b], B. Kiani[83a,83b], F. Legger[83a], F. Luongo[83a,83b], C. Mariotti[83a], L. Markovic[83a,83b], S. Maselli[83a], A. Mecca[83a,83b], L. Menzio[83a,83b], P. Meridiani[83a], E. Migliore[83a,83b], M. Monteno[83a], R. Mulargia[83a], M.M. Obertino[83a,83b], G. Ortona[83a], L. Pacher[83a,83b], N. Pastrone[83a], M. Pelliccioni[83a], M. Ruspa[83a,83c], F. Siviero[83a,83b], V. Sola[83a,83b], A. Solano[83a,83b], A. Staiano[83a], C. Tarricone[83a,83b], D. Trocino[83a], G. Umoret[83a,83b], R. White[83a,83b], J. Babbar[84a,84b], S. Belforte[84a], V. Candelise[84a,84b], M. Casarsa[84a], F. Cossutti[84a], K. De Leo[84a], G. Della Ricca[84a,84b], R. Delli Gatti[84a,84b], S. Dogra[85], J. Hong[85], B. Kim[85], J. Kim[85], D. Lee[85], H. Lee[85], S.W. Lee[85], C.S. Moon[85], Y.D. Oh[85], M.S. Ryu[85], S. Sekmen[85], B. Tae[85], Y.C. Yang[85], M.S. Kim[86], G. Bak[87], P. Gwak[87], H. Kim[87], D.H. Moon[87], E. Asilar[88], J. Choi[88,bd], D. Kim[88], T.J. Kim[88], J.A. Merlin[88], Y. Ryou[88], S. Choi[89], S. Han[89], B. Hong[89], K. Lee[89], K.S. Lee[89], S. Lee[89], J. Yoo[89], J. Goh[90], S. Yang[90], H. S. Kim[91], Y. Kim[91], S. Lee[91], J. Almond[92], J.H. Bhyun[92], J. Choi[92], J. Choi[92], W. Jun[92], J. Kim[92], Y.W. Kim[92], S. Ko[92], H. Kwon[92], H. Lee[92], J. Lee[92], J. Lee[92], B.H. Oh[92], S.B. Oh[92], H. Seo[92], U.K. Yang[92], I. Yoon[92], W. Jang[93], D.Y. Kang[93], Y. Kang[93], S. Kim[93], B. Ko[93], J.S.H. Lee[93], Y. Lee[93], I.C. Park[93], Y. Roh[93], I.J. Watson[93], S. Ha[94], K. Hwang[94], H.D. Yoo[94], M. Choi[95], M.R. Kim[95], H. Lee[95], Y. Lee[95], I. Yu[95], T. Beyrouthy[96], Y. Gharbia[96], K. Dreimanis[97], A. Gaile[97], C. Munoz Diaz[97], D. Osite[97], G. Pikurs[97], A. Potrebko[97], M. Seidel[97], D. Sidiropoulos Kontos[97], N.R. Strautnieks[98], M. Ambrozas[99], A. Juodagalvis[99], A. Rinkevicius[99], G. Tamulaitis[99], I. Yusuff[100,be], Z. Zolkapli[100], J.F. Benitez[101], A. Castaneda Hernandez[101], H.A. Encinas Acosta[101], L.G. Gallegos Maríñez[101], M. León Coello[101], J.A. Murillo Quijada[101], A. Sehrawat[101], L. Valencia Palomo[101], G. Ayala[102], H. Castilla-Valdez[102], H. Crotte Ledesma[102], E. De La Cruz-Burelo[102], I. Heredia-De La Cruz[102,bf], R. Lopez-Fernandez[102], J. Mejia Guisao[102], C.A. Mondragon Herrera[102], A. Sánchez Hernández[102], C. Oropeza Barrera[103], M. Ramírez García[103], D.L. Ramirez Guadarrama[103], I. Bautista[104], I. Pedraza[104], H.A. Salazar Ibarguen[104], C. Uribe Estrada[104], I. Bubanja[105], N. Raicevic[105], P.H. Butler[106], A. Ahmad[107], M.I. Asghar[107], A. Awais[107], M.I.M. Awan[107], H.R. Hoorani[107], W.A. Khan[107], V. Avati[108], L. Grzanka[108], M. Malawski[108],

H. Bialkowska[109], M. Bluj[109], M. Górski[109], M. Kazana[109], M. Szleper[109], P. Zalewski[109], K. Bunkowski[110], K. Doroba[110], A. Kalinowski[110], M. Konecki[110], J. Krolikowski[110], A. Muhammad[110], P. Fokow[111], K. Pozniak[111], W. Zabolotny[111], M. Araujo[112], D. Bastos[112], C. Beirão Da Cruz E Silva[112], A. Boletti[112], M. Bozzo[112], T. Camporesi[112], G. Da Molin[112], P. Faccioli[112], M. Gallinaro[112], J. Hollar[112], N. Leonardo[112], G.B. Marozzo[112], T. Niknejad[112], A. Petrilli[112], M. Pisano[112], J. Seixas[112], J. Varela[112], J.W. Wulff[112], P. Adzic[113], P. Milenovic[113], D. Devetak[114], M. Dordevic[114], J. Milosevic[114], L. Nadderd[114], V. Rekovic[114], J. Alcaraz Maestre[115], Cristina F. Bedoya[115], J.A. Brochero Cifuentes[115], Oliver M. Carretero[115], M. Cepeda[115], M. Cerrada[115], N. Colino[115], B. De La Cruz[115], A. Delgado Peris[115], A. Escalante Del Valle[115], D. Fernández Del Val[115], J.P. Fernández Ramos[115], J. Flix[115], M.C. Fouz[115], O. Gonzalez Lopez[115], S. Goy Lopez[115], J.M. Hernandez[115], M.I. Josa[115], J. Llorente Merino[115], E. Martin Viscasillas[115], D. Moran[115], C. M. Morcillo Perez[115], Á. Navarro Tobar[115], C. Perez Dengra[115], A. Pérez-Calero Yzquierdo[115], J. Puerta Pelayo[115], I. Redondo[115], S. Sánchez Navas[115], J. Sastre[115], J. Vazquez Escobar[115], J.F. de Trocóniz[116], B. Alvarez Gonzalez[117], J. Cuevas[117], J. Fernandez Menendez[117], S. Folgueras[117], I. Gonzalez Caballero[117], P. Leguina[117], E. Palencia Cortezon[117], J. Prado Pico[117], C. Ramón Álvarez[117], V. Rodríguez Bouza[117], A. Soto Rodríguez[117], A. Trapote[117], C. Vico Villalba[117], P. Vischia[117], S. Bhowmik[118], S. Blanco Fernández[118], I.J. Cabrillo[118], A. Calderon[118], J. Duarte Campderros[118], M. Fernandez[118], G. Gomez[118], C. Lasaosa García[118], R. Lopez Ruiz[118], C. Martinez Rivero[118], P. Martinez Ruiz del Arbol[118], F. Matorras[118], P. Matorras Cuevas[118], E. Navarrete Ramos[118], J. Piedra Gomez[118], L. Scodellaro[118], I. Vila[118], J.M. Vizan Garcia[118], B. Kailasapathy[119,bg], D.D.C. Wickramarathna[119], W.G.D. Dharmaratna[120,bh], K. Liyanage[120], N. Perera[120], D. Abbaneo[121], C. Amendola[121], E. Auffray[121], G. Auzinger[121], J. Baechler[121], D. Barney[121], A. Bermúdez Martínez[121], M. Bianco[121], A.A. Bin Anuar[121], A. Bocci[121], L. Borgonovi[121], C. Botta[121], E. Brondolin[121], C. Caillol[121], G. Cerminara[121], N. Chernyavskaya[121], D. d'Enterria[121], A. Dabrowski[121], A. David[121], A. De Roeck[121], M.M. Defranchis[121], M. Deile[121], M. Dobson[121], G. Franzoni[121], W. Funk[121], S. Giani[121], D. Gigi[121], K. Gill[121], F. Glege[121], J. Hegeman[121], J.K. Heikkilä[121], B. Huber[121], V. Innocente[121], T. James[121], P. Janot[121], O. Kaluzinska[121], O. Karacheban[121,ab], S. Laurila[121], P. Lecoq[121], E. Leutgeb[121], C. Lourenço[121], L. Malgeri[121], M. Mannelli[121], M. Matthewman[121], A. Mehta[121], F. Meijers[121], S. Mersi[121], E. Meschi[121], V. Milosevic[121], F. Monti[121], F. Moortgat[121], M. Mulders[121], I. Neutelings[121], S. Orfanelli[121], F. Pantaleo[121], G. Petrucciani[121], A. Pfeiffer[121], M. Pierini[121], H. Qu[121], D. Rabady[121], B. Ribeiro Lopes[121], F. Riti[121], M. Rovere[121], H. Sakulin[121], S. Sanchez Cruz[121], S. Scarfi[121], M. Selvaggi[121], A. Sharma[121], K. Shchelina[121], P. Silva[121], P. Sphicas[121,bi], A.G. Stahl Leiton[121], A. Steen[121], S. Summers[121], D. Treille[121], P. Tropea[121], D. Walter[121], J. Wanczyk[121,bj], J. Wang[121], K.A. Wozniak[121,bk], S. Wuchterl[121], P. Zehetner[121], P. Zejdl[121], W.D. Zeuner[121], T. Bevilacqua[122,bl], L. Caminada[122,bl], A. Ebrahimi[122], W. Erdmann[122], R. Horisberger[122], Q. Ingram[122], H.C. Kaestli[122], D. Kotlinski[122], C. Lange[122], M. Missiroli[122,bl], L. Noehte[122,bl], T. Rohe[122],

A. Samalan[122], T.K. Aarrestad[123], M. Backhaus[123], G. Bonomelli[123], A. Calandri[123], C. Cazzaniga[123], K. Datta[123], P. De Bryas Dexmiers D'archiac[123,bj], A. De Cosa[123], G. Dissertori[123], M. Dittmar[123], M. Donegà[123], F. Eble[123], M. Galli[123], K. Gedia[123], F. Glessgen[123], C. Grab[123], N. Härringer[123], T.G. Harte[123], D. Hits[123], W. Lustermann[123], A.-M. Lyon[123], R.A. Manzoni[123], M. Marchegiani[123], L. Marchese[123], C. Martin Perez[123], A. Mascellani[123,bj], F. Nessi-Tedaldi[123], F. Pauss[123], V. Perovic[123], S. Pigazzini[123], B. Ristic[123], R. Seidita[123], J. Steggemann[123,bj], A. Tarabini[123], D. Valsecchi[123], R. Wallny[123], C. Amsler[124,bm], P. Bärtschi[124], M.F. Canelli[124], K. Cormier[124], M. Huwiler[124], W. Jin[124], A. Jofrehei[124], B. Kilminster[124], S. Leontsinis[124], S.P. Liechti[124], A. Macchiolo[124], P. Meiring[124], F. Meng[124], U. Molinatti[124], J. Motta[124], A. Reimers[124], P. Robmann[124], M. Senger[124], E. Shokr[124], F. Stäger[124], R. Tramontano[124], C. Adloff[125,bn], D. Bhowmik[125], C.M. Kuo[125], W. Lin[125], P.K. Rout[125], P.C. Tiwari[125,am], L. Ceard[126], K.F. Chen[126], Z.g. Chen[126], A. De Iorio[126], W.-S. Hou[126], T.h. Hsu[126], Y.w. Kao[126], S. Karmakar[126], G. Kole[126], Y.y. Li[126], R.-S. Lu[126], E. Paganis[126], X.f. Su[126], J. Thomas-Wilsker[126], L.s. Tsai[126], D. Tsionou[126], H.y. Wu[126], E. Yazgan[126], C. Asawatangtrakuldee[127], N. Srimanobhas[127], V. Wachirapusitanand[127], D. Agyel[128], F. Boran[128], F. Dolek[128], I. Dumanoglu[128,bo], E. Eskut[128], Y. Guler[128,bp], E. Gurpinar Guler[128,bp], C. Isik[128], O. Kara[128], A. Kayis Topaksu[128], U. Kiminsu[128], Y. Komurcu[128], G. Onengut[128], K. Ozdemir[128,bq], A. Polatoz[128], B. Tali[128,br], U.G. Tok[128], S. Turkcapar[128], E. Uslan[128], I.S. Zorbakir[128], G. Sokmen[129], M. Yalvac[129,bs], B. Akgun[130], I.O. Atakisi[130], E. Gülmez[130], M. Kaya[130,bt], O. Kaya[130,bu], S. Tekten[130,bv], A. Cakir[131], K. Cankocak[131,bo,bw], G.G. Dincer[131,bo], S. Sen[131,bx], O. Aydilek[132,by], B. Hacisahinoglu[132], I. Hos[132,bz], B. Kaynak[132], S. Ozkorucuklu[132], O. Potok[132], H. Sert[132], C. Simsek[132], C. Zorbilmez[132], S. Cerci[133], B. Isildak[133,ca], D. Sunar Cerci[133], T. Yetkin[133], A. Boyaryntsev[134], B. Grynyov[134], L. Levchuk[135], D. Anthony[136], J.J. Brooke[136], A. Bundock[136], F. Bury[136], E. Clement[136], D. Cussans[136], H. Flacher[136], M. Glowacki[136], J. Goldstein[136], H.F. Heath[136], M.-L. Holmberg[136], L. Kreczko[136], S. Paramesvaran[136], L. Robertshaw[136], V.J. Smith[136], K. Walkingshaw Pass[136], A.H. Ball[137], K.W. Bell[137], A. Belyaev[137,cb], C. Brew[137], R.M. Brown[137], D.J.A. Cockerill[137], C. Cooke[137], A. Elliot[137], K.V. Ellis[137], K. Harder[137], S. Harper[137], J. Linacre[137], K. Manolopoulos[137], D.M. Newbold[137], E. Olaiya[137], D. Petyt[137], T. Reis[137], A.R. Sahasransu[137], G. Salvi[137], T. Schuh[137], C.H. Shepherd-Themistocleous[137], I.R. Tomalin[137], K.C. Whalen[137], T. Williams[137], I. Andreou[138], R. Bainbridge[138], P. Bloch[138], C.E. Brown[138], O. Buchmuller[138], C.A. Carrillo Montoya[138], G.S. Chahal[138,cc], D. Colling[138], J.S. Dancu[138], I. Das[138], P. Dauncey[138], G. Davies[138], M. Della Negra[138], S. Fayer[138], G. Fedi[138], G. Hall[138], A. Howard[138], G. Iles[138], C.R. Knight[138], P. Krueper[138], J. Langford[138], J. León Holgado[138], L. Lyons[138], A.-M. Magnan[138], B. Maier[138], S. Mallios[138], M. Mieskolainen[138], J. Nash[138,cd], M. Pesaresi[138], P.B. Pradeep[138], B.C. Radburn-Smith[138], A. Richards[138], A. Rose[138], K. Savva[138], C. Seez[138], R. Shukla[138], A. Tapper[138], K. Uchida[138], G.P. Uttley[138], L.H. Vage[138], T. Virdee[138,ae], M. Vojinovic[138], N. Wardle[138], D. Winterbottom[138], J.E. Cole[139], A. Khan[139], P. Kyberd[139], I.D. Reid[139], S. Abdullin[140], A. Brinkerhoff[140], E. Collins[140],

JHEP08(2026)049

M.R. Darwish[140], J. Dittmann[140], K. Hatakeyama[140], J. Hiltbrand[140], B. McMaster[140], J. Samudio[140], S. Sawant[140], C. Sutantawibul[140], J. Wilson[140], R. Bartek[141], A. Dominguez[141], A.E. Simsek[141], S.S. Yu[141], B. Bam[142], A. Buchot Perraguin[142], R. Chudasama[142], S.I. Cooper[142], C. Crovella[142], S.V. Gleyzer[142], E. Pearson[142], C.U. Perez[142], P. Rumerio[142,ce], E. Usai[142], R. Yi[142], A. Akpinar[143], C. Cosby[143], G. De Castro[143], Z. Demiragli[143], C. Erice[143], C. Fangmeier[143], C. Fernandez Madrazo[143], E. Fontanesi[143], D. Gastler[143], F. Golf[143], S. Jeon[143], J. O'cain[143], I. Reed[143], J. Rohlf[143], K. Salyer[143], D. Sperka[143], D. Spitzbart[143], I. Suarez[143], A. Tsatsos[143], A.G. Zecchinelli[143], G. Benelli[144], D. Cutts[144], L. Gouskos[144], M. Hadley[144], U. Heintz[144], J.M. Hogan[144,cf], T. Kwon[144], G. Landsberg[144], K.T. Lau[144], D. Li[144], J. Luo[144], S. Mondal[144], T. Russell[144], S. Sagir[144,cg], X. Shen[144], F. Simpson[144], M. Stamenkovic[144], N. Venkatasubramanian[144], X. Yan[144], S. Abbott[145], C. Brainerd[145], R. Breedon[145], H. Cai[145], M. Calderon De La Barca Sanchez[145], M. Chertok[145], M. Citron[145], J. Conway[145], P.T. Cox[145], R. Erbacher[145], F. Jensen[145], O. Kukral[145], G. Mocellin[145], M. Mulhearn[145], S. Ostrom[145], W. Wei[145], S. Yoo[145], F. Zhang[145], K. Adamidis[146], M. Bachtis[146], D. Campos[146], R. Cousins[146], A. Datta[146], G. Flores Avila[146], J. Hauser[146], M. Ignatenko[146], M.A. Iqbal[146], T. Lam[146], Y.f. Lo[146], E. Manca[146], A. Nunez Del Prado[146], D. Saltzberg[146], V. Valuev[146], R. Clare[147], J.W. Gary[147], M. Gordon[147], G. Hanson[147], W. Si[147], A. Aportela[148], A. Arora[148], J.G. Branson[148], S. Cittolin[148], S. Cooperstein[148], D. Diaz[148], J. Duarte[148], L. Giannini[148], Y. Gu[148], J. Guiang[148], R. Kansal[148], V. Krutelyov[148], R. Lee[148], J. Letts[148], M. Masciovecchio[148], F. Mokhtar[148], S. Mukherjee[148], M. Pieri[148], M. Quinnan[148], B.V. Sathia Narayanan[148], V. Sharma[148], M. Tadel[148], E. Vourliotis[148], F. Würthwein[148], Y. Xiang[148], A. Yagil[148], A. Barzdukas[149], L. Brennan[149], C. Campagnari[149], K. Downham[149], C. Grieco[149], J. Incandela[149], J. Kim[149], A.J. Li[149], P. Masterson[149], H. Mei[149], J. Richman[149], S.N. Santpur[149], U. Sarica[149], R. Schmitz[149], F. Setti[149], J. Sheplock[149], D. Stuart[149], T.Á. Vámi[149], S. Wang[149], D. Zhang[149], S. Bhattacharya[150], A. Bornheim[150], O. Cerri[150], A. Latorre[150], J. Mao[150], H.B. Newman[150], G. Reales Gutiérrez[150], M. Spiropulu[150], J.R. Vlimant[150], C. Wang[150], S. Xie[150], R.Y. Zhu[150], J. Alison[151], S. An[151], P. Bryant[151], M. Cremonesi[151], V. Dutta[151], T. Ferguson[151], T.A. Gómez Espinosa[151], A. Harilal[151], A. Kallil Tharayil[151], C. Liu[151], T. Mudholkar[151], S. Murthy[151], P. Palit[151], K. Park[151], M. Paulini[151], A. Roberts[151], A. Sanchez[151], W. Terrill[151], J.P. Cumalat[152], W.T. Ford[152], A. Hart[152], A. Hassani[152], G. Karathanasis[152], N. Manganelli[152], J. Pearkes[152], C. Savard[152], N. Schonbeck[152], K. Stenson[152], K.A. Ulmer[152], S.R. Wagner[152], N. Zipper[152], D. Zuolo[152], J. Alexander[153], S. Bright-Thonney[153], X. Chen[153], D.J. Cranshaw[153], J. Fan[153], X. Fan[153], S. Hogan[153], P. Kotamnives[153], J. Monroy[153], M. Oshiro[153], J.R. Patterson[153], M. Reid[153], A. Ryd[153], J. Thom[153], P. Wittich[153], R. Zou[153], M. Albrow[154], M. Alyari[154], O. Amram[154], G. Apollinari[154], A. Apresyan[154], L.A.T. Bauerdick[154], D. Berry[154], J. Berryhill[154], P.C. Bhat[154], K. Burkett[154], J.N. Butler[154], A. Canepa[154], G.B. Cerati[154], H.W.K. Cheung[154], F. Chlebana[154], G. Cummings[154], J. Dickinson[154], I. Dutta[154], V.D. Elvira[154], Y. Feng[154], J. Freeman[154], A. Gandrakota[154], Z. Gecse[154], L. Gray[154], D. Green[154], A. Grummer[154],

S. Grünendahl[154], D. Guerrero[154], O. Gutsche[154], R.M. Harris[154], R. Heller[154], T.C. Herwig[154], J. Hirschauer[154], B. Jayatilaka[154], S. Jindariani[154], M. Johnson[154], U. Joshi[154], T. Klijnsma[154], B. Klima[154], K.H.M. Kwok[154], S. Lammel[154], C. Lee[154], D. Lincoln[154], R. Lipton[154], T. Liu[154], C. Madrid[154], K. Maeshima[154], C. Mantilla[154], D. Mason[154], P. McBride[154], P. Merkel[154], S. Mrenna[154], S. Nahn[154], J. Ngadiuba[154], D. Noonan[154], S. Norberg[154], V. Papadimitriou[154], N. Pastika[154], K. Pedro[154], C. Pena[154,ch], F. Ravera[154], A. Reinsvold Hall[154,ci], L. Ristori[154], M. Safdari[154], E. Sexton-Kennedy[154], N. Smith[154], A. Soha[154], L. Spiegel[154], S. Stoynev[154], J. Strait[154], L. Taylor[154], S. Tkaczyk[154], N.V. Tran[154], L. Uplegger[154], E.W. Vaandering[154], I. Zoi[154], C. Aruta[155], P. Avery[155], D. Bourilkov[155], P. Chang[155], V. Cherepanov[155], R.D. Field[155], C. Huh[155], E. Koenig[155], M. Kolosova[155], J. Konigsberg[155], A. Korytov[155], K. Matchev[155], N. Menendez[155], G. Mitselmakher[155], K. Mohrman[155], A. Muthirakalayil Madhu[155], N. Rawal[155], S. Rosenzweig[155], Y. Takahashi[155], J. Wang[155], T. Adams[156], A. Al Kadhim[156], A. Askew[156], S. Bower[156], R. Hashmi[156], R.S. Kim[156], S. Kim[156], T. Kolberg[156], G. Martinez[156], H. Prosper[156], P.R. Prova[156], M. Wulansatiti[156], R. Yohay[156], J. Zhang[156], B. Alsufyani[157], M.M. Baarmand[157], S. Butalla[157], S. Das[157], T. Elkafrawy[157,q], M. Hohlmann[157], E. Yanes[157], M.R. Adams[158], A. Baty[158], C. Bennett[158], R. Cavanaugh[158], R. Escobar Franco[158], O. Evdokimov[158], C.E. Gerber[158], M. Hawksworth[158], A. Hingrajiya[158], D.J. Hofman[158], J.h. Lee[158], D. S. Lemos[158], A.H. Merrit[158], C. Mills[158], S. Nanda[158], G. Oh[158], B. Ozek[158], D. Pilipovic[158], R. Pradhan[158], E. Prifti[158], T. Roy[158], S. Rudrabhatla[158], N. Singh[158], M.B. Tonjes[158], N. Varelas[158], M.A. Wadud[158], Z. Ye[158], J. Yoo[158], M. Alhusseini[159], D. Blend[159], K. Dilsiz[159,cj], L. Emediato[159], G. Karaman[159], O.K. Köseyan[159], J.-P. Merlo[159], A. Mestvirishvili[159,ck], O. Neogi[159], H. Ogul[159,cl], Y. Onel[159], A. Penzo[159], C. Snyder[159], E. Tiras[159,cm], B. Blumenfeld[160], L. Corcodilos[160], J. Davis[160], A.V. Gritsan[160], L. Kang[160], S. Kyriacou[160], P. Maksimovic[160], M. Roguljic[160], J. Roskes[160], S. Sekhar[160], M. Swartz[160], A. Abreu[161], L.F. Alcerro Alcerro[161], J. Anguiano[161], S. Arteaga Escatel[161], P. Baringer[161], A. Bean[161], Z. Flowers[161], D. Grove[161], J. King[161], G. Krintiras[161], M. Lazarovits[161], C. Le Mahieu[161], J. Marquez[161], M. Murray[161], M. Nickel[161], M. Pitt[161], S. Popescu[161,cn], C. Rogan[161], C. Royon[161], R. Salvatico[161], S. Sanders[161], C. Smith[161], G. Wilson[161], B. Allmond[162], R. Gujju Gurunadha[162], A. Ivanov[162], K. Kaadze[162], Y. Maravin[162], J. Natoli[162], D. Roy[162], G. Sorrentino[162], A. Baden[163], A. Belloni[163], J. Bistany-riebman[163], Y.M. Chen[163], S.C. Eno[163], N.J. Hadley[163], S. Jabeen[163], R.G. Kellogg[163], T. Koeth[163], B. Kronheim[163], Y. Lai[163], S. Lascio[163], A.C. Mignerey[163], S. Nabili[163], C. Palmer[163], C. Papageorgakis[163], M.M. Paranjpe[163], E. Popova[163,co], A. Shevelev[163], L. Wang[163], J. Bendavid[164], I.A. Cali[164], P.c. Chou[164], M. D'Alfonso[164], J. Eysermans[164], C. Freer[164], G. Gomez-Ceballos[164], M. Goncharov[164], G. Grosso[164], P. Harris[164], D. Hoang[164], D. Kovalskyi[164], J. Krupa[164], L. Lavezzo[164], Y.-J. Lee[164], K. Long[164], C. Mcginn[164], A. Novak[164], M.I. Park[164], C. Paus[164], C. Reissel[164], C. Roland[164], G. Roland[164], S. Rothman[164], G.S.F. Stephans[164], Z. Wang[164], B. Wyslouch[164], T. J. Yang[164], B. Crossman[165], B.M. Joshi[165], C. Kapsiak[165], M. Krohn[165], D. Mahon[165], J. Mans[165], B. Marzocchi[165],

JHEP08(2026)049

M. Revering[165], R. Rusack[165], R. Saradhy[165], N. Strobbe[165], K. Bloom[166], D.R. Claes[166], G. Haza[166], J. Hossain[166], C. Joo[166], I. Kravchenko[166], J.E. Siado[166], W. Tabb[166], A. Vagnerini[166], A. Wightman[166], F. Yan[166], D. Yu[166], H. Bandyopadhyay[167], L. Hay[167], H.w. Hsia[167], I. Iashvili[167], A. Kalogeropoulos[167], A. Kharchilava[167], M. Morris[167], D. Nguyen[167], S. Rappoccio[167], H. Rejeb Sfar[167], A. Williams[167], P. Young[167], G. Alverson[168], E. Barberis[168], J. Bonilla[168], B. Bylsma[168], M. Campana[168], J. Dervan[168], Y. Haddad[168], Y. Han[168], I. Israr[168], A. Krishna[168], J. Li[168], M. Lu[168], G. Madigan[168], R. Mccarthy[168], D.M. Morse[168], V. Nguyen[168], T. Orimoto[168], A. Parker[168], L. Skinnari[168], D. Wood[168], J. Bueghly[169], S. Dittmer[169], K.A. Hahn[169], Y. Liu[169], M. Mcginnis[169], Y. Miao[169], D.G. Monk[169], M.H. Schmitt[169], A. Taliercio[169], M. Velasco[169], G. Agarwal[170], R. Band[170], R. Bucci[170], S. Castells[170], A. Das[170], R. Goldouzian[170], M. Hildreth[170], K.W. Ho[170], K. Hurtado Anampa[170], T. Ivanov[170], C. Jessop[170], K. Lannon[170], J. Lawrence[170], N. Loukas[170], L. Lutton[170], J. Mariano[170], N. Marinelli[170], I. Mcalister[170], T. McCauley[170], C. Mcgrady[170], C. Moore[170], Y. Musienko[170,o], H. Nelson[170], M. Osherson[170], A. Piccinelli[170], R. Ruchti[170], A. Townsend[170], Y. Wan[170], M. Wayne[170], H. Yockey[170], M. Zarucki[170], L. Zygala[170], A. Basnet[171], M. Carrigan[171], L.S. Durkin[171], C. Hill[171], M. Joyce[171], M. Nunez Ornelas[171], K. Wei[171], B.L. Winer[171], B. R. Yates[171], H. Bouchamaoui[172], K. Coldham[172], P. Das[172], G. Dezoort[172], P. Elmer[172], A. Frankenthal[172], B. Greenberg[172], N. Haubrich[172], K. Kennedy[172], G. Kopp[172], S. Kwan[172], D. Lange[172], A. Loeliger[172], D. Marlow[172], I. Ojalvo[172], J. Olsen[172], D. Stickland[172], C. Tully[172], S. Malik[173], R. Sharma[173], A.S. Bakshi[174], S. Chandra[174], R. Chawla[174], A. Gu[174], L. Gutay[174], M. Jones[174], A.W. Jung[174], A.M. Koshy[174], M. Liu[174], G. Negro[174], N. Neumeister[174], G. Paspalaki[174], S. Piperov[174], V. Scheurer[174], J.F. Schulte[174], M. Stojanovic[174], J. Thieman[174], A. K. Virdi[174], F. Wang[174], A. Wildridge[174], W. Xie[174], Y. Yao[174], J. Dolen[175], N. Parashar[175], A. Pathak[175], D. Acosta[176], T. Carnahan[176], K.M. Ecklund[176], P.J. Fernández Manteca[176], S. Freed[176], P. Gardner[176], F.J.M. Geurts[176], I. Krommydas[176], W. Li[176], J. Lin[176], O. Miguel Colin[176], B.P. Padley[176], R. Redjimi[176], J. Rotter[176], E. Yigitbasi[176], Y. Zhang[176], A. Bodek[177], P. de Barbaro[177], R. Demina[177], J.L. Dulemba[177], A. Garcia-Bellido[177], O. Hindrichs[177], A. Khukhunaishvili[177], N. Parmar[177], P. Parygin[177,co], R. Taus[177], B. Chiarito[178], J.P. Chou[178], S.V. Clark[178], D. Gadkari[178], Y. Gershtein[178], E. Halkiadakis[178], M. Heindl[178], C. Houghton[178], D. Jaroslawski[178], S. Konstantinou[178], I. Laflotte[178], A. Lath[178], R. Montalvo[178], K. Nash[178], J. Reichert[178], H. Routray[178], P. Saha[178], S. Salur[178], S. Schnetzer[178], S. Somalwar[178], R. Stone[178], S.A. Thayil[178], S. Thomas[178], J. Vora[178], H. Wang[178], D. Ally[179], A.G. Delannoy[179], S. Fiorendi[179], S. Higginbotham[179], T. Holmes[179], A.R. Kanuganti[179], N. Karunarathna[179], L. Lee[179], E. Nibigira[179], S. Spanier[179], D. Aebi[180], M. Ahmad[180], T. Akhter[180], K. Androsov[180,bj], O. Bouhali[180,cp], R. Eusebi[180], J. Gilmore[180], T. Huang[180], T. Kamon[180,cq], H. Kim[180], S. Luo[180], R. Mueller[180], D. Overton[180], D. Rathjens[180], A. Safonov[180], N. Akchurin[181], J. Damgov[181], N. Gogate[181], V. Hegde[181], A. Hussain[181], Y. Kazhykarim[181], K. Lamichhane[181], S.W. Lee[181], A. Mankel[181], T. Peltola[181], I. Volobouev[181], E. Appelt[182], Y. Chen[182], S. Greene[182], A. Gurrola[182], W. Johns[182],

R. Kunnawalkam Elayavalli[182], A. Melo[182], F. Romeo[182], P. Sheldon[182], S. Tuo[182], J. Velkovska[182], J. Viinikainen[182], B. Cardwell[183], H. Chung[183], B. Cox[183], J. Hakala[183], R. Hirosky[183], A. Ledovskoy[183], C. Neu[183], S. Bhattacharya[184], P.E. Karchin[184], A. Aravind[185], S. Banerjee[185], K. Black[185], T. Bose[185], E. Chavez[185], S. Dasu[185], I. De Bruyn[185], P. Everaerts[185], C. Galloni[185], H. He[185], M. Herndon[185], A. Herve[185], C.K. Koraka[185], A. Lanaro[185], R. Loveless[185], J. Madhusudanan Sreekala[185], A. Mallampalli[185], A. Mohammadi[185], S. Mondal[185], G. Parida[185], L. Pétré[185], D. Pinna[185], A. Savin[185], V. Shang[185], V. Sharma[185], W.H. Smith[185], D. Teague[185], H.F. Tsoi[185], W. Vetens[185], A. Warden[185], S. Afanasiev[186], V. Alexakhin[186], D. Budkouski[186], I. Golutvin[186,†], I. Gorbunov[186], V. Karjavine[186], V. Korenkov[186], A. Lanev[186], A. Malakhov[186], V. Matveev[186,o], V. Palichik[186], V. Perelygin[186], M. Savina[186], V. Shalaev[186], S. Shmatov[186], S. Shulha[186], V. Smirnov[186], O. Teryaev[186], N. Voytishin[186], B.S. Yuldashev[186,cr], A. Zarubin[186], I. Zhizhin[186], V. Andreev[187], Yu. Andreev[187], T. Aushev[187], M. Azarkin[187], A. Babaev[187], V. Blinov[187,o], E. Boos[187], V. Borshch[187], V. Bunichev[187], V. Chekhovsky[187], R. Chistov[187,o], M. Danilov[187,o], A. Dermenev[187], T. Dimova[187,o], D. Druzhkin[187], M. Dubinin[187,ch], L. Dudko[187], G. Gavrilov[187], V. Gavrilov[187], S. Gninenko[187], V. Golovtcov[187], N. Golubev[187], Y. Ivanov[187], V. Kachanov[187], A. Karneyeu[187], V. Kim[187,o], M. Kirakosyan[187], D. Kirpichnikov[187], M. Kirsanov[187], V. Klyukhin[187], O. Kodolova[187,cs], D. Konstantinov[187], A. Kozyrev[187,o], N. Krasnikov[187], P. Levchenko[187,ct], O. Lukina[187], N. Lychkovskaya[187], V. Makarenko[187], V. Murzin[187], A. Nikitenko[187,cu,cv], S. Obraztsov[187], V. Oreshkin[187], M. Perfilov[187], S. Polikarpov[187,o], V. Popov[187], O. Radchenko[187,o], V. Savrin[187], Y. Skovpen[187,o], S. Slabospitskii[187], A. Snigirev[187], D. Sosnov[187], V. Sulimov[187], A. Terkulov[187], I. Tlisova[187], A. Toropin[187], L. Uvarov[187], A. Uzunian[187], A. Vorobyev[187,†], G. Vorotnikov[187], A. Zhokin[187]

[1] *Yerevan Physics Institute, Yerevan, Armenia*
[2] *Institut für Hochenergiephysik, Vienna, Austria*
[3] *Universiteit Antwerpen, Antwerpen, Belgium*
[4] *Vrije Universiteit Brussel, Brussel, Belgium*
[5] *Université Libre de Bruxelles, Bruxelles, Belgium*
[6] *Ghent University, Ghent, Belgium*
[7] *Université Catholique de Louvain, Louvain-la-Neuve, Belgium*
[8] *Centro Brasileiro de Pesquisas Fisicas, Rio de Janeiro, Brazil*
[9] *Universidade do Estado do Rio de Janeiro, Rio de Janeiro, Brazil*
[10] *Universidade Estadual Paulista, Universidade Federal do ABC, São Paulo, Brazil*
[11] *Institute for Nuclear Research and Nuclear Energy, Bulgarian Academy of Sciences, Sofia, Bulgaria*
[12] *University of Sofia, Sofia, Bulgaria*
[13] *Instituto De Alta Investigación, Universidad de Tarapacá, Casilla 7 D, Arica, Chile*
[14] *Beihang University, Beijing, China*
[15] *Department of Physics, Tsinghua University, Beijing, China*
[16] *Institute of High Energy Physics, Beijing, China*
[17] *State Key Laboratory of Nuclear Physics and Technology, Peking University, Beijing, China*
[18] *State Key Laboratory of Nuclear Physics and Technology, Institute of Quantum Matter, South China Normal University, Guangzhou, China*
[19] *Sun Yat-Sen University, Guangzhou, China*
[20] *University of Science and Technology of China, Hefei, China*
[21] *Nanjing Normal University, Nanjing, China*

JHEP08(2026)049

[22] *Institute of Modern Physics and Key Laboratory of Nuclear Physics and Ion-beam Application (MOE) - Fudan University, Shanghai, China*
[23] *Zhejiang University, Hangzhou, Zhejiang, China*
[24] *Universidad de Los Andes, Bogota, Colombia*
[25] *Universidad de Antioquia, Medellin, Colombia*
[26] *University of Split, Faculty of Electrical Engineering, Mechanical Engineering and Naval Architecture, Split, Croatia*
[27] *University of Split, Faculty of Science, Split, Croatia*
[28] *Institute Rudjer Boskovic, Zagreb, Croatia*
[29] *University of Cyprus, Nicosia, Cyprus*
[30] *Charles University, Prague, Czech Republic*
[31] *Universidad San Francisco de Quito, Quito, Ecuador*
[32] *Academy of Scientific Research and Technology of the Arab Republic of Egypt, Egyptian Network of High Energy Physics, Cairo, Egypt*
[33] *Center for High Energy Physics (CHEP-FU), Fayoum University, El-Fayoum, Egypt*
[34] *National Institute of Chemical Physics and Biophysics, Tallinn, Estonia*
[35] *Department of Physics, University of Helsinki, Helsinki, Finland*
[36] *Helsinki Institute of Physics, Helsinki, Finland*
[37] *Lappeenranta-Lahti University of Technology, Lappeenranta, Finland*
[38] *IRFU, CEA, Université Paris-Saclay, Gif-sur-Yvette, France*
[39] *Laboratoire Leprince-Ringuet, CNRS/IN2P3, Ecole Polytechnique, Institut Polytechnique de Paris, Palaiseau, France*
[40] *Université de Strasbourg, CNRS, IPHC UMR 7178, Strasbourg, France*
[41] *Centre de Calcul de l'Institut National de Physique Nucleaire et de Physique des Particules, CNRS/IN2P3, Villeurbanne, France*
[42] *Institut de Physique des 2 Infinis de Lyon (IP2I), Villeurbanne, France*
[43] *Georgian Technical University, Tbilisi, Georgia*
[44] *RWTH Aachen University, I. Physikalisches Institut, Aachen, Germany*
[45] *RWTH Aachen University, III. Physikalisches Institut A, Aachen, Germany*
[46] *RWTH Aachen University, III. Physikalisches Institut B, Aachen, Germany*
[47] *Deutsches Elektronen-Synchrotron, Hamburg, Germany*
[48] *University of Hamburg, Hamburg, Germany*
[49] *Karlsruher Institut fuer Technologie, Karlsruhe, Germany*
[50] *Institute of Nuclear and Particle Physics (INPP), NCSR Demokritos, Aghia Paraskevi, Greece*
[51] *National and Kapodistrian University of Athens, Athens, Greece*
[52] *National Technical University of Athens, Athens, Greece*
[53] *University of Ioánnina, Ioánnina, Greece*
[54] *HUN-REN Wigner Research Centre for Physics, Budapest, Hungary*
[55] *MTA-ELTE Lendület CMS Particle and Nuclear Physics Group, Eötvös Loránd University, Budapest, Hungary*
[56] *Faculty of Informatics, University of Debrecen, Debrecen, Hungary*
[57] *HUN-REN ATOMKI - Institute of Nuclear Research, Debrecen, Hungary*
[58] *Karoly Robert Campus, MATE Institute of Technology, Gyongyos, Hungary*
[59] *Panjab University, Chandigarh, India*
[60] *University of Delhi, Delhi, India*
[61] *Saha Institute of Nuclear Physics, HBNI, Kolkata, India*
[62] *Indian Institute of Technology Madras, Madras, India*
[63] *Tata Institute of Fundamental Research-A, Mumbai, India*
[64] *Tata Institute of Fundamental Research-B, Mumbai, India*
[65] *National Institute of Science Education and Research, An OCC of Homi Bhabha National Institute, Bhubaneswar, Odisha, India*
[66] *Indian Institute of Science Education and Research (IISER), Pune, India*
[67] *Isfahan University of Technology, Isfahan, Iran*

JHEP08(2026)049

[68] *Institute for Research in Fundamental Sciences (IPM), Tehran, Iran*
[69] *University College Dublin, Dublin, Ireland*
[70a] *INFN Sezione di Bari, Bari, Italy*
[70b] *Università di Bari, Bari, Italy*
[70c] *Politecnico di Bari, Bari, Italy*
[71a] *INFN Sezione di Bologna, Bologna, Italy*
[71b] *Università di Bologna, Bologna, Italy*
[72a] *INFN Sezione di Catania, Catania, Italy*
[72b] *Università di Catania, Catania, Italy*
[73a] *INFN Sezione di Firenze, Firenze, Italy*
[73b] *Università di Firenze, Firenze, Italy*
[74] *INFN Laboratori Nazionali di Frascati, Frascati, Italy*
[75a] *INFN Sezione di Genova, Genova, Italy*
[75b] *Università di Genova, Genova, Italy*
[76a] *INFN Sezione di Milano-Bicocca, Milano, Italy*
[76b] *Università di Milano-Bicocca, Milano, Italy*
[77a] *INFN Sezione di Napoli, Napoli, Italy*
[77b] *Università di Napoli 'Federico II', Napoli, Italy*
[77c] *Università della Basilicata, Potenza, Italy*
[77d] *Scuola Superiore Meridionale (SSM), Napoli, Italy*
[78a] *INFN Sezione di Padova, Padova, Italy*
[78b] *Università di Padova, Padova, Italy*
[78c] *Universita degli Studi di Cagliari, Cagliari, Italy*
[79a] *INFN Sezione di Pavia, Pavia, Italy*
[79b] *Università di Pavia, Pavia, Italy*
[80a] *INFN Sezione di Perugia, Perugia, Italy*
[80b] *Università di Perugia, Perugia, Italy*
[81a] *INFN Sezione di Pisa, Pisa, Italy*
[81b] *Università di Pisa, Pisa, Italy*
[81c] *Scuola Normale Superiore di Pisa, Pisa, Italy*
[81d] *Università di Siena, Siena, Italy*
[82a] *INFN Sezione di Roma, Roma, Italy*
[82b] *Sapienza Università di Roma, Roma, Italy*
[83a] *INFN Sezione di Torino, Torino, Italy*
[83b] *Università di Torino, Torino, Italy*
[83c] *Università del Piemonte Orientale, Novara, Italy*
[84a] *INFN Sezione di Trieste, Trieste, Italy*
[84b] *Università di Trieste, Trieste, Italy*
[85] *Kyungpook National University, Daegu, Korea*
[86] *Department of Mathematics and Physics - GWNU, Gangneung, Korea*
[87] *Chonnam National University, Institute for Universe and Elementary Particles, Kwangju, Korea*
[88] *Hanyang University, Seoul, Korea*
[89] *Korea University, Seoul, Korea*
[90] *Kyung Hee University, Department of Physics, Seoul, Korea*
[91] *Sejong University, Seoul, Korea*
[92] *Seoul National University, Seoul, Korea*
[93] *University of Seoul, Seoul, Korea*
[94] *Yonsei University, Department of Physics, Seoul, Korea*
[95] *Sungkyunkwan University, Suwon, Korea*
[96] *College of Engineering and Technology, American University of the Middle East (AUM), Dasman, Kuwait*
[97] *Riga Technical University, Riga, Latvia*
[98] *University of Latvia (LU), Riga, Latvia*
[99] *Vilnius University, Vilnius, Lithuania*

[100] *National Centre for Particle Physics, Universiti Malaya, Kuala Lumpur, Malaysia*
[101] *Universidad de Sonora (UNISON), Hermosillo, Mexico*
[102] *Centro de Investigacion y de Estudios Avanzados del IPN, Mexico City, Mexico*
[103] *Universidad Iberoamericana, Mexico City, Mexico*
[104] *Benemerita Universidad Autonoma de Puebla, Puebla, Mexico*
[105] *University of Montenegro, Podgorica, Montenegro*
[106] *University of Canterbury, Christchurch, New Zealand*
[107] *National Centre for Physics, Quaid-I-Azam University, Islamabad, Pakistan*
[108] *AGH University of Krakow, Krakow, Poland*
[109] *National Centre for Nuclear Research, Swierk, Poland*
[110] *Institute of Experimental Physics, Faculty of Physics, University of Warsaw, Warsaw, Poland*
[111] *Warsaw University of Technology, Warsaw, Poland*
[112] *Laboratório de Instrumentação e Física Experimental de Partículas, Lisboa, Portugal*
[113] *Faculty of Physics, University of Belgrade, Belgrade, Serbia*
[114] *VINCA Institute of Nuclear Sciences, University of Belgrade, Belgrade, Serbia*
[115] *Centro de Investigaciones Energéticas Medioambientales y Tecnológicas (CIEMAT), Madrid, Spain*
[116] *Universidad Autónoma de Madrid, Madrid, Spain*
[117] *Universidad de Oviedo, Instituto Universitario de Ciencias y Tecnologías Espaciales de Asturias (ICTEA), Oviedo, Spain*
[118] *Instituto de Física de Cantabria (IFCA), CSIC-Universidad de Cantabria, Santander, Spain*
[119] *University of Colombo, Colombo, Sri Lanka*
[120] *University of Ruhuna, Department of Physics, Matara, Sri Lanka*
[121] *CERN, European Organization for Nuclear Research, Geneva, Switzerland*
[122] *PSI Center for Neutron and Muon Sciences, Villigen, Switzerland*
[123] *ETH Zurich - Institute for Particle Physics and Astrophysics (IPA), Zurich, Switzerland*
[124] *Universität Zürich, Zurich, Switzerland*
[125] *National Central University, Chung-Li, Taiwan*
[126] *National Taiwan University (NTU), Taipei, Taiwan*
[127] *High Energy Physics Research Unit, Department of Physics, Faculty of Science, Chulalongkorn University, Bangkok, Thailand*
[128] *Çukurova University, Physics Department, Science and Art Faculty, Adana, Turkey*
[129] *Middle East Technical University, Physics Department, Ankara, Turkey*
[130] *Bogazici University, Istanbul, Turkey*
[131] *Istanbul Technical University, Istanbul, Turkey*
[132] *Istanbul University, Istanbul, Turkey*
[133] *Yildiz Technical University, Istanbul, Turkey*
[134] *Institute for Scintillation Materials of National Academy of Science of Ukraine, Kharkiv, Ukraine*
[135] *National Science Centre, Kharkiv Institute of Physics and Technology, Kharkiv, Ukraine*
[136] *University of Bristol, Bristol, U.K.*
[137] *Rutherford Appleton Laboratory, Didcot, U.K.*
[138] *Imperial College, London, U.K.*
[139] *Brunel University, Uxbridge, U.K.*
[140] *Baylor University, Waco, Texas, U.S.A.*
[141] *Catholic University of America, Washington, DC, U.S.A.*
[142] *The University of Alabama, Tuscaloosa, Alabama, U.S.A.*
[143] *Boston University, Boston, Massachusetts, U.S.A.*
[144] *Brown University, Providence, Rhode Island, U.S.A.*
[145] *University of California, Davis, Davis, California, U.S.A.*
[146] *University of California, Los Angeles, California, U.S.A.*
[147] *University of California, Riverside, Riverside, California, U.S.A.*
[148] *University of California, San Diego, La Jolla, California, U.S.A.*
[149] *University of California, Santa Barbara - Department of Physics, Santa Barbara, California, U.S.A.*
[150] *California Institute of Technology, Pasadena, California, U.S.A.*

JHEP08(2026)049

[151] *Carnegie Mellon University, Pittsburgh, Pennsylvania, U.S.A.*
[152] *University of Colorado Boulder, Boulder, Colorado, U.S.A.*
[153] *Cornell University, Ithaca, New York, U.S.A.*
[154] *Fermi National Accelerator Laboratory, Batavia, Illinois, U.S.A.*
[155] *University of Florida, Gainesville, Florida, U.S.A.*
[156] *Florida State University, Tallahassee, Florida, U.S.A.*
[157] *Florida Institute of Technology, Melbourne, Florida, U.S.A.*
[158] *University of Illinois Chicago, Chicago, Illinois, U.S.A.*
[159] *The University of Iowa, Iowa City, Iowa, U.S.A.*
[160] *Johns Hopkins University, Baltimore, Maryland, U.S.A.*
[161] *The University of Kansas, Lawrence, Kansas, U.S.A.*
[162] *Kansas State University, Manhattan, Kansas, U.S.A.*
[163] *University of Maryland, College Park, Maryland, U.S.A.*
[164] *Massachusetts Institute of Technology, Cambridge, Massachusetts, U.S.A.*
[165] *University of Minnesota, Minneapolis, Minnesota, U.S.A.*
[166] *University of Nebraska-Lincoln, Lincoln, Nebraska, U.S.A.*
[167] *State University of New York at Buffalo, Buffalo, New York, U.S.A.*
[168] *Northeastern University, Boston, Massachusetts, U.S.A.*
[169] *Northwestern University, Evanston, Illinois, U.S.A.*
[170] *University of Notre Dame, Notre Dame, Indiana, U.S.A.*
[171] *The Ohio State University, Columbus, Ohio, U.S.A.*
[172] *Princeton University, Princeton, New Jersey, U.S.A.*
[173] *University of Puerto Rico, Mayaguez, Puerto Rico, U.S.A.*
[174] *Purdue University, West Lafayette, Indiana, U.S.A.*
[175] *Purdue University Northwest, Hammond, Indiana, U.S.A.*
[176] *Rice University, Houston, Texas, U.S.A.*
[177] *University of Rochester, Rochester, New York, U.S.A.*
[178] *Rutgers, The State University of New Jersey, Piscataway, New Jersey, U.S.A.*
[179] *University of Tennessee, Knoxville, Tennessee, U.S.A.*
[180] *Texas A&M University, College Station, Texas, U.S.A.*
[181] *Texas Tech University, Lubbock, Texas, U.S.A.*
[182] *Vanderbilt University, Nashville, Tennessee, U.S.A.*
[183] *University of Virginia, Charlottesville, Virginia, U.S.A.*
[184] *Wayne State University, Detroit, Michigan, U.S.A.*
[185] *University of Wisconsin - Madison, Madison, Wisconsin, U.S.A.*
[186] *An institute or international laboratory covered by a cooperation agreement with CERN*
[187] *An institute formerly covered by a cooperation agreement with CERN*

[a] *Also at Yerevan State University, Yerevan, Armenia*
[b] *Also at TU Wien, Vienna, Austria*
[c] *Also at Ghent University, Ghent, Belgium*
[d] *Also at Universidade do Estado do Rio de Janeiro, Rio de Janeiro, Brazil*
[e] *Also at Universidade Estadual de Campinas, Campinas, Brazil*
[f] *Also at Federal University of Rio Grande do Sul, Porto Alegre, Brazil*
[g] *Also at UFMS, Nova Andradina, Brazil*
[h] *Also at University of Chinese Academy of Sciences, Beijing, China*
[i] *Also at China Center of Advanced Science and Technology, Beijing, China*
[j] *Also at University of Chinese Academy of Sciences, Beijing, China*
[k] *Also at China Spallation Neutron Source, Guangdong, China*
[l] *Now at Henan Normal University, Xinxiang, China*
[m] *Also at University of Shanghai for Science and Technology, Shanghai, China*
[n] *Now at The University of Iowa, Iowa City, Iowa, U.S.A.*
[o] *Also at Another institute formerly covered by a cooperation agreement with CERN*

JHEP08(2026)049

[p] Also at Cairo University, Cairo, Egypt
[q] Also at Ain Shams University, Cairo, Egypt
[r] Also at Suez University, Suez, Egypt
[s] Now at British University in Egypt, Cairo, Egypt
[t] Also at Purdue University, West Lafayette, Indiana, U.S.A.
[u] Also at Université de Haute Alsace, Mulhouse, France
[v] Also at Istinye University, Istanbul, Turkey
[w] Also at Another institute or international laboratory covered by a cooperation agreement with CERN
[x] Also at The University of the State of Amazonas, Manaus, Brazil
[y] Also at University of Hamburg, Hamburg, Germany
[z] Also at RWTH Aachen University, III. Physikalisches Institut A, Aachen, Germany
[aa] Also at Bergische University Wuppertal (BUW), Wuppertal, Germany
[ab] Also at Brandenburg University of Technology, Cottbus, Germany
[ac] Also at Forschungszentrum Jülich, Juelich, Germany
[ad] Now at RWTH Aachen University, III. Physikalisches Institut A, Aachen, Germany
[ae] Also at CERN, European Organization for Nuclear Research, Geneva, Switzerland
[af] Also at HUN-REN ATOMKI - Institute of Nuclear Research, Debrecen, Hungary
[ag] Now at Universitatea Babes-Bolyai - Facultatea de Fizica, Cluj-Napoca, Romania
[ah] Also at MTA-ELTE Lendület CMS Particle and Nuclear Physics Group, Eötvös Loránd University, Budapest, Hungary
[ai] Also at HUN-REN Wigner Research Centre for Physics, Budapest, Hungary
[aj] Also at Physics Department, Faculty of Science, Assiut University, Assiut, Egypt
[ak] Also at Punjab Agricultural University, Ludhiana, India
[al] Also at University of Visva-Bharati, Santiniketan, India
[am] Also at Indian Institute of Science (IISc), Bangalore, India
[an] Also at IIT Bhubaneswar, Bhubaneswar, India
[ao] Also at Institute of Physics, Bhubaneswar, India
[ap] Also at University of Hyderabad, Hyderabad, India
[aq] Also at Deutsches Elektronen-Synchrotron, Hamburg, Germany
[ar] Also at Isfahan University of Technology, Isfahan, Iran
[as] Also at Sharif University of Technology, Tehran, Iran
[at] Also at Department of Physics, University of Science and Technology of Mazandaran, Behshahr, Iran
[au] Also at Department of Physics, Faculty of Science, Arak University, ARAK, Iran
[av] Also at Helwan University, Cairo, Egypt
[aw] Also at Italian National Agency for New Technologies, Energy and Sustainable Economic Development, Bologna, Italy
[ax] Also at Centro Siciliano di Fisica Nucleare e di Struttura Della Materia, Catania, Italy
[ay] Also at Università degli Studi Guglielmo Marconi, Roma, Italy
[az] Also at Scuola Superiore Meridionale, Università di Napoli 'Federico II', Napoli, Italy
[ba] Also at Fermi National Accelerator Laboratory, Batavia, Illinois, U.S.A.
[bb] Also at Lulea University of Technology, Lulea, Sweden
[bc] Also at Consiglio Nazionale delle Ricerche - Istituto Officina dei Materiali, Perugia, Italy
[bd] Also at Institut de Physique des 2 Infinis de Lyon (IP2I), Villeurbanne, France
[be] Also at Department of Applied Physics, Faculty of Science and Technology, Universiti Kebangsaan Malaysia, Bangi, Malaysia
[bf] Also at Consejo Nacional de Ciencia y Tecnología, Mexico City, Mexico
[bg] Also at Trincomalee Campus, Eastern University, Sri Lanka, Nilaveli, Sri Lanka
[bh] Also at Saegis Campus, Nugegoda, Sri Lanka
[bi] Also at National and Kapodistrian University of Athens, Athens, Greece
[bj] Also at Ecole Polytechnique Fédérale Lausanne, Lausanne, Switzerland
[bk] Also at University of Vienna, Vienna, Austria
[bl] Also at Universität Zürich, Zurich, Switzerland
[bm] Also at Stefan Meyer Institute for Subatomic Physics, Vienna, Austria

JHEP08(2026)049

[bn] Also at Laboratoire d'Annecy-le-Vieux de Physique des Particules, IN2P3-CNRS, Annecy-le-Vieux, France
[bo] Also at Near East University, Research Center of Experimental Health Science, Mersin, Turkey
[bp] Also at Konya Technical University, Konya, Turkey
[bq] Also at Izmir Bakircay University, Izmir, Turkey
[br] Also at Adiyaman University, Adiyaman, Turkey
[bs] Also at Bozok Universitetesi Rektörlügü, Yozgat, Turkey
[bt] Also at Marmara University, Istanbul, Turkey
[bu] Also at Milli Savunma University, Istanbul, Turkey
[bv] Also at Kafkas University, Kars, Turkey
[bw] Now at Istanbul Okan University, Istanbul, Turkey
[bx] Also at Hacettepe University, Ankara, Turkey
[by] Also at Erzincan Binali Yildirim University, Erzincan, Turkey
[bz] Also at Istanbul University - Cerrahpasa, Faculty of Engineering, Istanbul, Turkey
[ca] Also at Yildiz Technical University, Istanbul, Turkey
[cb] Also at School of Physics and Astronomy, University of Southampton, Southampton, U.K.
[cc] Also at IPPP Durham University, Durham, U.K.
[cd] Also at Monash University, Faculty of Science, Clayton, Australia
[ce] Also at Università di Torino, Torino, Italy
[cf] Also at Bethel University, St. Paul, Minnesota, U.S.A.
[cg] Also at Karamanoğlu Mehmetbey University, Karaman, Turkey
[ch] Also at California Institute of Technology, Pasadena, California, U.S.A.
[ci] Also at United States Naval Academy, Annapolis, Maryland, U.S.A.
[cj] Also at Bingol University, Bingol, Turkey
[ck] Also at Georgian Technical University, Tbilisi, Georgia
[cl] Also at Sinop University, Sinop, Turkey
[cm] Also at Erciyes University, Kayseri, Turkey
[cn] Also at Horia Hulubei National Institute of Physics and Nuclear Engineering (IFIN-HH), Bucharest, Romania
[co] Now at Another institute formerly covered by a cooperation agreement with CERN
[cp] Also at Texas A&M University at Qatar, Doha, Qatar
[cq] Also at Kyungpook National University, Daegu, Korea
[cr] Also at Institute of Nuclear Physics of the Uzbekistan Academy of Sciences, Tashkent, Uzbekistan
[cs] Also at Yerevan Physics Institute, Yerevan, Armenia
[ct] Also at Northeastern University, Boston, Massachusetts, U.S.A.
[cu] Also at Imperial College, London, U.K.
[cv] Now at Yerevan Physics Institute, Yerevan, Armenia
[†] Deceased